KERNFORSCHUNGSZENTRUM

KARLSRUHE

Juni 1976 KFK 2286

Abteilung Strahlenschutz und Sicherheit
Projekt Nukleare Sicherheit

Experimental Determination of the Atmospheric Dispersion Parameters over Rough Terrain
Part 2
Evaluation of Measurements

P. Thomas, K. Nester

GESELLSCHAFT
FÜR
KERNFORSCHUNG M.B.H.

KARLSRUHE

KERNFORSCHUNGSZENTRUM KARLSRUHE

KFK 2286

Abteilung Strahlenschutz und Sicherheit
Projekt Nukleare Sicherheit

Experimental Determination of the Atmospheric Dispersion Parameters over Rough Terrain

Part 2

Evaluation of Measurements

P. Thomas
K. Nester

Gesellschaft für Kernforschung m.b.H., Karlsruhe

Abstract

Experiments are carried out at the Karlsruhe Nuclear Research Center in order to determine the atmospheric diffusion of pollutants. The influence on atmospheric diffusion by topographic conditions specific to the site is to be investigated.

For evaluation of the measurements the diffusion is assumed to be a steady state process. A two dimensional Gaussian distribution is used as the theoretical approximation of the concentrations. The dependence of the dispersion parameters σ_y and σ_z on the distance from the source is described by a power function. The least squares technique is applied to assess the horizontal and vertical dispersion parameters and the normalized diffusion factor with the respective errors.

The parameters determined in this way are compared with those according to Pasquill/Gifford. Relative to these families of curves a shift towards instability can be found. This shift is most pronounced under neutral diffusion conditions and is insignificant in unstable conditions. Moreover, the horizontal dispersion parameters have a flatter slope in a log-log diagram than those according to Pasquill/Gifford.

In Part 1 of this report (KFK 2285) the diffusion experiments are described and the measured data are presented in a detailed manner.

Zusammenfassung

Experimentelle Bestimmung der atmosphärischen Ausbreitungsparameter über rauhem Gelände

Teil 2

Auswertung der Meßergebnisse

Am Kernforschungszentrum Karlsruhe werden Experimente durchgeführt, um die Ausbreitung von Schadstoffen in der Atmosphäre zu erforschen. Standortspezifische Einflüsse sollen dabei untersucht werden.

Mittels der Methode der kleinsten Fehlerquadrate werden aus der gemessenen Konzentrationsverteilung die horizontalen und vertikalen Ausbreitungsparameter und der normierte Ausbreitungsfaktor sowie die zugehörigen Fehlerbreiten ermittelt. Für die Konzentration wird eine zweidimensionale Gaußverteilung zugrunde gelegt. Die Ausbreitung wird als stationär angenommen. Ein Potenzansatz beschreibt die Abhängigkeit der Ausbreitungsparameter von der Quelldistanz.

Die ermittelten Parameter werden mit denjenigen nach Pasquill/Gifford verglichen. Dabei ist gegenüber den Kurvenscharen nach Pasquill/Gifford eine Verschiebung nach labil festzustellen. Die Verschiebung ist am stärksten bei neutralen Ausbreitungsbedingungen und nur unbedeutend bei labilen Lagen. Außerdem haben die horizontalen Ausbreitungsparameter in der doppelt logarithmischen Darstellung eine geringere Neigung als diejenigen nach Pasquill/Gifford.

Im ersten Teil dieses Berichtes (KFK 2285) werden die Ausbreitungsexperimente beschrieben und die Meßergebnisse in Form von Tabellen ausführlich dargestellt.

Table of Contents

1. Introduction

For reliable estimates of the environmental pollution caused by airborne pollutants the mechanism of atmospheric diffusion must be known. Topographic conditions specific to a site exert a considerable influence on atmospheric diffusion. For this reason, experimental verification of the relations between meteorological conditions and the parameters determining diffusion is necessary for various sites. A test program has been carried out at the Karlsruhe Nuclear Research Center for many years with the purpose of determining dispersion parameters under different meteorological conditions and demonstrating the influences specific to the site by comparing with the familiar parameter curves according to Pasquill/Gifford /1/, /2/.

The results of measurements compiled in the first part of this paper /3/ are evaluated by the least squares method.

Some results of the experiments performed so far have already been published in /4/, /5/, /6/, /7/, /8/, /9/, /10/. The dispersion parameters shown here are the results achieved so far in an experimental program not yet finished.

If extremely non-steady state conditions prevailed during the experiments, they were not treated by this method. The theoretical model chosen is not suitable to these cases.

2. Evaluation Technique

The concentration distributions at ground level measured in the diffusion experiments were used to determine the dispersion parameters for this purpose. The least squares technique is applied to adapt the theoretical distribution to the concentrations measured.

2.1 Theoretical Distribution

The theoretical expression for the concentration close to the ground level downwind of the source at the field point P(x,y) reads

$$C(x,y) = \frac{\chi_n(x,y)\,\dot{A}_0}{u} = \frac{\dot{A}_0}{\pi\,u\,\sigma_y(x)\,\sigma_z(x)}\exp\left[-\frac{y^2}{2\,\sigma_y^2(x)}-\frac{H^2}{2\,\sigma_z^2(x)}\right]. \qquad (1)$$

This follows from the diffusion equation for steady state conditions, constant emission rate and reflection of the tracer at ground level, where

$\dot{A}_o$ emission rate in Ci/s or g/s,
u mean wind velocitiy in m/s,
$\chi_n(x,y)$ normalized diffusion factor in m^{-2},
x local coordinate in the transport direction in m,
y horizontal local coordinate perpendicular to the transport direction in m,
H emission height in m,
σ_y, σ_z horizontal and vertical dispersion parameters, respectively, in m.

The foot of the source lies in the point of origin of the Cartesian coordinate system.

2.2 Dispersion Parameters

The dispersion parameters σ_y and σ_z describe the horizontal and vertical distributions of the concentration perpendicular to the transport direction, respectively. They are a function of the distance x from the source.

For this dependence on x, the power functions

$$\sigma_y = \sigma_{oy}\, x^{p_y}, \quad \sigma_z = \sigma_{oz}\, x^{p_z} \tag{2}$$

are chosen.

2.3 Least Squares Method

The measured values C_i determined at field points with coordinates x_i and y_i are available ($i = 1, 2 \ldots, n$; $n \geq 4$). A weight g_i is assigned to each measured value.

Four parameters $q_j(\sigma_{oy}, p_y, \sigma_{oz}, p_z)$ must be found to fit the function $f(x,y,\overline{q})$ to the measured values in such a way that the sum of the square deviations,

$$Q = \sum_{i=1}^{n} g_i(f_i - C_i)^2 \tag{3}$$

becomes a minimum.

$$f_i = f(x_i, y_i, \overline{q}) \tag{4}$$

The vector $\overline{q}$ stands for the four parameters q_j, and $f(x,y,\overline{q})$ for $C(x,y)$ from equation (1).

In order to minimize the sum Q,

$$\frac{\partial Q}{\partial q_j} = 0 \text{ for } j = 1,2,3,4 \tag{5}$$

must hold.

These are four equations determining the four parameters q_j. Since the function f is not a linear function of the parameters q_j, an approximation technique with iterative improvement must be applied to solve (5).

For the parameters it is postulated that

$$q_j = q_{oj} + \delta q_j. \tag{6}$$

In a first approximation

$$f(x,y,\overline{q}) = f(x,y,\overline{q_o}) + \sum_{j=1}^{4} \frac{\partial f(x,y,\overline{q_o})}{\partial q_{oj}} \delta q_j . \tag{7}$$

If (7) is substituted in (3), (5) supplies a system of linear equations:

$$\frac{\partial Q}{\partial \delta q_m} = 2 \sum_{i=1}^{n} g_i \left[f_i(\overline{q_o}) + \sum_{j=1}^{4} \frac{\partial f_i(\overline{q_o})}{\partial q_{oj}} \delta q_j - C_i \right] \frac{\partial f_i(\overline{q_o})}{\partial q_{om}} = 0 \tag{8}$$

or

$$\sum_{j=1}^{4} N_{jm}\, \delta q_j = -\sum_{i=1}^{n} g_i \left[f_i(\overline{q_o}) - C_i \right] \frac{\partial f_i(\overline{q_o})}{\partial q_{om}} \quad , m = 1, 2, 3, 4 \quad (9)$$

for determining δq_j.

For this purpose, the standard matrix

$$N_{jm} = \sum_{i=1}^{n} g_i \frac{\partial f_i(\overline{q_o})}{\partial q_{oj}} \frac{\partial f_i(\overline{q_o})}{\partial q_{om}} \quad (10)$$

must not be singular.

The improved parameters

$$q_{1j} = q_{oj} + \delta q_j \quad (11)$$

are substituted in the function f. They are improved by further iteration steps. This process is continued until the change ΔQ of the sum of the square deviations between two iteration steps is less than an optional value.

For better convergence, a damping factor $\beta < 1$ is introduced:

$$q_{rj} = q_{(r-1)j} + \beta^S \delta q_{rj}, \quad (12)$$

where r is the r^{th}-iteration step. After each iteration step the sum of the square deviations Q_r is calculated and compared with Q_{r-1}. For S it holds that

$S = 0$ for $Q_r < Q_{r-1}$,
$S = 1$ for $Q_r > Q_{r-1}$.

Next, another comparison is made. If $Q_r > Q_{r-1}$ still holds, S will be increased by 1. This is continued, until $Q_r < Q_{r-1}$ or a given number of damping steps has been achieved.

2.4 Error Considerations

The inverse standard matrix

$$I_{j,m} = (N_{j,m})^{-1}$$

can be used to determine the errors of the parameters q_j and the errors of any functions of the parameters. The error of the parameter is

$$\Delta q_j = R \sqrt{I_{jj}} \tag{13}$$

The error Δh of any function $h(\overline{q})$ is

$$\Delta h = R \sqrt{\sum_{j=1}^{4} \sum_{m=1}^{4} \frac{\partial h(\overline{q})}{\partial q_j} I_{jm} \frac{\partial h(\overline{q})}{\partial q_m}} , \tag{14}$$

where

$$R = \sqrt{\frac{Q}{n-4}} , \tag{15}$$

which is the square root of the reduced sum of the least squares. In calculating the error, the values q_j resulting from the fit are used for R and I_{jm}. The errors in the dispersion parameters σ_y and σ_z are calculated according to (14). They qualify the fit and, hence, the reliability of the calculated dispersion parameters. The errors are caused by the scattering of the measured values around the theoretical curve and are due to changes in wind direction and variations between open spaces, built up and wooded areas within the test field. The error in measurement is hardly significant.

2.5 Weighting and Initial Approximations

First computer runs showed a disadvantage of the evaluation technique. If different first approximations q_{oj} are used, the same concentration distribution gave rise to different parameters q_j. But the dispersion parameters showed good agreement at distances of maximum concentrations. The respective sums of least squares differed only slightly in most cases. To avoid this effect each measured value is weighted in such a way that the contribution to the sum of the square deviations is independent of distance. This weighting prefers low measured values at near and remote distances.

In computer evaluation initially all concentration values of the same zone (cf. /3/) are weighted equally. The weighting factor in a zone is the ratio between the maximum concentration of all sampling locations and the maximum concentration within the respective zone. In a following run each concentration is weighted individually with

$$g_i = C_{max}/C(x_i,0) . \qquad (16)$$

C_{max} is the maximum value of all values $C(x_i,0)$. In Equation (16) the dispersion parameters σ_y, σ_z, which have been determined in each previous run, are then taken into account. This iteration process is continued until the change in parameters between two succeeding steps is less than an optional value.

Despite the weighting, different ensembles q_{oj} are used for each evaluation which are taken from the families of curves according to Pasquill/Gifford /1/, /2/. If different results were still found, that ensemble q_j is deemed to be representative whose least squares sum Q is the smallest.

2.6 Transport Direction

The best fit to the measured concentrations can be reached, if transport directions are chosen which differ slightly from the directions traced by the wind vane. For this reason, several computer runs are always carried out varying the transport direction in steps of 1^o. Again, that direction is deemed to be representative whose respective least squares sum is the smallest. The difference between the direction of transport obtained from the experiments and measured on the tower in some cases exceeds 10^o.

2.7 Absorption

The absorption can be taken into account in expression (1) by an emission rate $\dot{A}(x)$ decreasing with the distance x. Simple terms are found for no absorption (reflection) at ground level: $\dot{A}(x) = \dot{A}_o$, and

total absorption at ground level: $\dot{A}(x) = \dot{A}_o \operatorname{erf}\left(\frac{H}{\sqrt{2}\,\sigma_z(x)}\right)$,

where

$$\operatorname{erf}(w) = \frac{2}{\sqrt{\pi}} \int_0^w \exp(-v^2)\,dv. \qquad (17)$$

$\dot{A}_o$ is the true emission rate used already in expression (1) and kept constant throughout the experiment.

As outlined above, the least squares method is used to determine the coefficients σ_{yo}, σ_{zo}, p_y, p_z for an assumed total absorption.

3. Evaluation

3.1 Experiments Suited for Evaluation

The concentrations measured in some of the sampling periods do not furnish physically meaningful solutions by the technique described in this paper. This happens if only the background concentration or the wings of the lateral distribution were measured, because of changes in the wind direction. It also applies to periods in which several zones show two peaks of concentration or where there is more than one peak in the direction of transport. During these periods extremely non-steady state conditions prevailed which are not taken into account in the diffusion model employed. For these cases a non-steady state model is being prepared /12/.

In some of the first experiments the number of sampling locations with sufficiently high concentrations was too low to be evaluated by the technique described above.

3.2 Wind Velocity and Source Height

In Equation (1) the wind velocity taken into account is measured at 60 m altitude at the tower, averaged over the sampling time. In the experiments the tracer was released from the 100 m high stack of the MZFR or FR2 reactor. The plume rise caused by the exit velocity compensates for the shift in the zero point due to the vegetation and justifies an effective emission height of 100 m.

3.3 Combination of Several Sampling Periods and Experiments

In order to obtain more reliable results,several periods are combined. For this purpose, the results of the evaluation of individual periods are used as a basis.

For the combination each period is weighted in proportion with the reciprocal value of the root R of the reduced least squares sum that resulted from the individual evaluations (cf. Relation 15). This weighting prefers periods whose respective dispersion parameters show small error widths. The optimum transport directions as determined in the individual evaluations are also taken into account. The combination is performed by treating the different periods as one period. The number of concentration values is increased by a factor equal to the number of combined periods. Of course, such combination is possible only for periods of equal diffusion category.

4. Presentation of the Dispersion Parameters Determined

Table 1 shows the coefficients σ_{oy}, σ_{oz}, p_y, p_z as determined and the dispersion parameters σ_y and σ_z with the respective error widths at three distances from the source for all sampling periods suited for evaluation. The three distances roughly represent the shortest and the longest distances of the sampling locations from the source and that distance at which the maximum concentration is found. The parameters obtained in a combination of several periods of an experiment (cf. Section 3.3) are also indicated.

In addition Table 1 contains the diffusion category prevailing during the experiment and the difference between the measured and the evaluated transport direction (cf. Section 2.6).

Figs. 1 to 75 show the dispersion parameters σ_y, σ_z and the normalized diffusion factor χ_n as a function of the distance x from the source (cf. Relation 1). All periods suited for evaluation of one experiment are combined. The error widths are plotted, too. For comparison, the corresponding curves according to Pasquill/Gifford are drawn as dashed lines.

Where several experiments could be assigned to the same category, mean dispersion parameters were calculated (cf. Section 3.3) which are summarized in Table 2. The arrangement is similar to that shown in Table 1. The dispersion parameters σ_y, σ_z and the normalized diffusion factors χ_n are also plotted in Figs. 76 to 87.

For Experiment 15 the results obtained for the reflection and total absorption model (cf. Section 2.7) are contrasted in Table 3. The square roots R of the reduced least squares sum are also indicated. In order to facilitate the comparison Figs. 88 and 89 show the parameters σ_y and σ_z as a function of the distance x from the source for all periods combined of Experiment 15 with the error widths.

5. Discussion of Results

Local topography plays a major role in assessing the results of diffusion experiments. The site near the source is plane, but a highly structured surface is produced by the buildings and the trees. Evaluations of the wind profile at the meteorological tower of 200 m height supplied a roughness length of 1.10 m /14/.

The curves of the two dispersion parameters σ_y and σ_z and of the diffusion factor χ_n were based upon the families of Pasquill-Gifford curves /1/, /2/, because these curves have so far been used to calculate environmental burdens in nuclear technology /15/. In the experiments constituting the main basis of Pasquill-Gifford's curves the tracer was emitted at low altitude over a plane surface with low roughness length ($z_0 \approx 0.01$ m). Because of the different topographical conditions no agreement was to be expected between our results and the curves by Pasquill and Gifford. However, on the basis of the found differences the surface effects can be interpreted more easily. For this reason, it was necessary to classify the meteorological conditions prevailing during the experiments in accordance with Pasquill's diffusion categories A - F. In this method of evaluation the roughness of the ground is not taken into account.

5.1 The Curves of the Vertical Dispersion Parameter σ_z

With a few exceptions, the σ_z curves determined in various experiments fit into the family of Pasquill-Gifford curves. Only the extreme rise in Pasquill-Gifford's curves for longer distances in categories A and B does not correspond to our results. The steep rise in the curves by Pasquill and Gifford is probably due to the low source height used in the underlying experiments. If this factor is taken into account, an assignment of our curves to the curves by Pasquill and Gifford can be made in accordance with Table 4.

In making the assignment in Table 4 not only the slope of the calculated curve, but also its error width was taken into account.

It appears from Table 4 that the results of Experiments 1 to 7 do not agree well with those of other experiments. The first experiments 1 - 7 were carried out with a small number of measuring points irregularly distributed and for this reason cannot be evaluated with the same weight as later experiments. They show that at least 25 measuring points are required at a site as heterogeneous as that of the Karlsruhe Nuclear Research Center.

The results of the experiments can be summarized as in Table 5.

The σ_z curve in category E is supported by only one experiment. In category E the assignment for this reason has no sufficiently firm basis. All experiments under D were carried out in the daytime. For this reason, they cannot be representative of the entire category D. In D-conditions at night turbulence intensities are lower, which requires a lower diffusion parameter σ_z. Hence, the category D should be assigned to the Pasquill/Gifford curve for B/C.

In summary it can be said that the experimentally determined σ_z curves for the site of the Karlsruhe Nuclear Research Center are displaced towards the unstable side relative to the corresponding Pasquill/Gifford curves. This shift is most pronounced in category D and is a minimum for categories A and B. This can be explained by an intensified mechanical turbulence due to increased roughness of the terrain. The mechanical turbulence is most pronounced in category D. In categories A and B, however, which are mainly characterized by thermal turbulence, the increase in mechanical turbulence has but a minor effect.

Since several experiments were already available for categories B, C and D_T, the respective experiments were summarized. The result is shown in Figs. 76 to 79.

On the basis of the assignment of our results to the Pasquill-Gifford curves it was attempted in /16/ to generalize the influence of roughness upon the dispersion parameter σ_z as a function of the diffusion categories by a theoretical and empirical approach. Assignments corresponding to Table 4 are indicated for 3 roughness classes.

5.2 The Curves of the Horizontal Dispersion Parameter σ_y

Local Conditions influence the dispersion very close to the ground and, hence, also the concentration distribution measured at 1 m above ground between buildings, on pathways in the forests and forest clearings. These topographical factors are reflected more clearly in σ_y than in σ_z, for the concentration distribution has a more direct bearing upon the calculation of σ_y. While in the σ_z curves a graduation corresponding to the diffusion categories could be observed, this is not seen in the σ_y curves (see Figs. 26 to 50). In most cases the slopes of the calculated σ_y curves are less than those of the Pasquill-Gifford curves. As the σ_z values, also the σ_y values are higher than the corresponding curves according to Pasquill-Gifford. For the σ_y curves this applies above all in the short distance range. For the rest, the error widths are mostly larger than in the σ_z curves.

For better valuation of the results, the experiments carried out under categories B, C and D_T, respectively, were summarized and are represented in Figs. 80 to 83. Unlike the results of Pasquill and Gifford, the slopes of the σ_y curves determined from several experiments differ in the unstable and neutral categories.

Compared with the curves according to Pasquill and Gifford the σ_y values are increased not only by the higher mechanical turbulence, but also by the structure of the site. This is true in particular in the short distance area around the source.

5.3 The Normalized Diffusion Factor χ_n

The diffusion factor χ_n gives an overview of the maximum pollutant burden to be expected from short time emissions. Since σ_z has a stronger influence upon the χ_n curve than σ_y, the same statements hold true for categories D_T and C as for σ_z. However, for the unstable categories A and B the increase in σ_y is markedly higher than for σ_z when compared with the curves of Pasquill-Gifford. For this reason, the respective χ_n curves in general are below the χ_n curves according to Pasquill-Gifford. A summary of the experiments in which categories B, C and D_T respectively, prevailed indicates this situation (see Figs. 84-87).

5.4 Absorption

In the theoretical setup for the evaluation, reflection at ground level was assumed. However, the topography on the site of the Karlsruhe Nuclear Research Center may act as a sink because in the forest the tracer participates in the diffusion with retardation because of the low transport velocity. However, the measurements are not directly influenced by sinks, because the points of measurement are not located in dense forest. In addition, when tritiated water vapor is used as the tracer, absorption by plants may occur /11/.

These effects can be considered by absorption on the ground. For Experiment 15 the maximum influence on the dispersion parameters was investigated by assuming total absorption (see Section 2.8). In Fig. 88 the σ_z curves for reflection and total absorption on the ground are contrasted with each other. As was to be expected, the σ_z curve has a flatter slope in the case of absorption than in the case of reflection. However, the shift towards the unstable side relative to the corresponding curves according to Pasquill and Gifford remains. Accordingly, it is not due to absorption effects but, as has been mentioned above, to the differences in roughness.

The power functions (2) and the coupling of the dispersion parameters by relation (1) also influence the curve of σ_y as shown in Fig. 89.

When evaluating Experiment 15, the error widths of σ_y and σ_z in the absorption and the reflection model don't differ significantly. Accordingly, it cannot be decided which of the models is the better one. Therefore, the consideration of absorption effects requires additional studies.

6. Final Remarks

The results of the experiments performed so far are in qualitative agreement with those carried out at St. Louis /17/ and Jülich /18/. They are not yet sufficient to set up a complete family of dispersion parameters for calculating the impact of pollutants over rough terrain. In particular, experiments carried out during categories D, E and F at night are still missing. They will be feasible only with an automated sampling system, which will be available in 1976. Since the influence of roughness is a function of the altitude, also experiments with different source heights (60 m, 160 m, 200 m) are to be carried out.

References

/1/ Pasquill,F.: Atmospheric Diffusion. London 1968

/2/ Hilsmeier, W.F., Gifford, L.A.: Graphs for Estimating Atmospheric Dispersion. ORO-545 (1962)

/3/ Thomas, P., Hübschmann, W., König, L.A., Schüttelkopf, H., Vogt, S., Winter, M.:Experimental Determination of the Atmospheric Dispersion Parameters over Rough Terrain. Part 1: Measurements at the Karlsruhe Nuclear Research Center. KFK 2285 (1976)

/4/ Comper, W., Hübschmann, W., Nester, K. in Jahresbericht 1970 der Abteilung Strahlenschutz und Sicherheit, KFK 1365 (1971), pp. 161

/5/ Hübschmann, W., König, L.A., Kropp, L., Nester, K., Schüttelkopf, H., Winter, M. in Jahresbericht 1971 der Abteilung Strahlenschutz und Sicherheit, KFK 1565 (1972), pp. 133

/6/ Hiller, J., König, L.A., Schüttelkopf, H., Winter, M. in Jahresbericht 1972 der Abteilung Strahlenschutz und Sicherheit, KFK 1818 (1973), pp. 141

/7/ Nester, K., Thomas, P. in Jahresbericht 1973 der Abteilung Strahlenschutz und Sicherheit. KFK 1973 (1974), pp. 134

/8/ König, L.A., Nester, K., Schüttelkopf, H., Winter, M.: Experiments Conducted at the Karlsruhe Nuclear Research Center to determine Diffusion in the Atmosphere by Means of Various Tracers.
Proceedings of the IAEA-Symposium on "Physical Behaviour of Radioactive Contaminants in the Atmosphere". Vienna 1974, pp. 67

/9/ Nester, K., Thomas, P.: Experimente zur Bestimmung der lokalen atmosphärischen Ausbreitung von Schadstoffen. KFK Nachrichten 6/2 (1974), pp. 28

/10/ Schüttelkopf, H., Thomas, P. in Jahresbericht 1974 der Abteilung Strahlenschutz und Sicherheit. KFK 2155 (1975), pp. 122

/11/ Kline, J.R., Stewart, M.L.: Tritium Uptake and Loss in Grass Vegetation which has been Exposed to an Atmospheric Source of Tritiated Water. Health Physics 26 (1974), pp. 567

/12/ Nester, K. in Jahresbericht 1971 der Abteilung Strahlenschutz und Sicherheit. KFK 1565 (1972), pp. 162

/13/ Nester, K.: Statistische Auswertungen der Windmessungen im Kernforschungszentrum Karlsruhe aus den Jahren 1968/69. KFK 1606 (1972)

/14/ Dilger, H., Nester, K., Vogt, S.: Statistische Auswertungen des Wind-, Temperatur- und Feuchteprofils sowie der Strahlung und der Windrichtungsfluktuation am Kernforschungszentrums Karlsruhe. KFK 2266 (1975)

/15/ Gifford, F.A.: An Outline of Theories of Diffusion in the Lower Layers of the Atmosphere. Meteorology and Atomic Energy, TID - 24190 (1968), pp. 65

/16/ Nester, K.: Abschätzung des Einflusses der Rauhigkeit auf die Diffusionsparameter für verschiedene Stabilitätszustände der Atmosphäre (accepted by Staub - Reinhaltung der Luft)

/17/ Vogt, K.J.: Kurzzeit- und Langzeitausbreitungsfaktoren zur Berechnung der Umweltbelastung durch Abluftfahnen. KFA-Jülich, ZST-Bericht Nr. 198, (1974)

/18/ Mc. Elrog, J.: A Comparative Study of Urban and Rural Dispersion, J.of.Appl.Met. 8/1 (1969), pp. 19

Table 1 Determined Dispersion Parameters

Nr.	Period	Tracer	Δφ	Category	y σ_0	y p	z σ_0	z p	x [m]	σ_y [m]	$\frac{\Delta\sigma_y}{\sigma_y}$ [%]	σ_z [m]	$\frac{\Delta\sigma_z}{\sigma_z}$ [%]
1	1	HTO	2^o	D	1,87	0,51	0,39	0,67	800	56	85	35	15
									2400	97	31	73	24
									4900	140	37	119	46
3	2	HTO	2^o	C	6,17	0,50	0,0017	1,54	1000	194	139	72	225
									2000	275	33	208	76
									3000	337	56	389	40
	3		13^o		0,55	0,92	0,011	1,25	1000	314	28	62	14
									2000	592	15	146	19
									3000	859	42	242	37
					5,61	0,56	0,0018	1,51	1000	261	21	62	11
									2000	384	17	176	19
									3000	481	29	325	27
6	1	HTO	11^o	C	0,0013	1,49	0,0015	1,49	1400	64	30	77	86
									2000	108	57	131	40
									4400	349	153	424	157
	2		16^o		0,12	0,89	0,62	0,60	1400	73	195	48	62
									2000	100	112	59	23
									4400	202	81	95	95
	3		1^o		0,25	0,79	0,45	0,65	1400	77	71	50	33
									2000	102	46	63	30
									4400	190	29	105	156
	4		4^o		0,084	0,89	1,14	0,54	1400	53	124	57	84
									2000	73	81	69	122
									4400	146	32	106	550
	5		6^o		0,013	1,40	5,43	0,50	1400	33	48	204	29
									2000	54	22	244	15
									4400	164	48	362	29
	6		13^o		1,15	0,65	1,23	0,56	1400	123	77	71	85
									2000	155	38	87	37
									4400	258	69	135	144
					0,027	1,08	7,05	0,46	1400	67	35	191	38
									2000	98	21	225	23
									4400	229	31	322	27
7	2	HTO	14^o	D	0,15	0,90	0,043	1,00	900	69	44	53	42
									1500	110	17	90	21
									2900	199	26	179	31
	3		14^o		0,013	1,25	0,0017	1,51	900	65	37	49	34
									1500	123	14	106	15
									2900	281	24	287	22
	4		14^o		0,068	1,01	2,40	0,44	900	65	27	47	19
									1500	108	14	58	8
									2900	210	18	77	18

Table 1 Continued

Nr.	Period	Tracer	Δφ	Category	y σ_0	y p	z σ_0	z p	x [m]	σ_y [m]	$\frac{\Delta\sigma_y}{\sigma_y}$ [%]	σ_z [m]	$\frac{\Delta\sigma_z}{\sigma_z}$ [%]
7	5	HTO	11°	D	0,40	0,82	0,0011	1,52	900	105	64	34	10
									1500	160	25	74	22
									2900	274	42	200	49
					3,06	0,53	0,0015	1,50	900	112	20	40	5
									1500	147	8	86	6
									2900	208	14	231	15
8	3	HTO	9°	C	3,98	0,48	5,79	0,85	700	94	19	1533	16
									1000	112	17	2077	15
									2000	156	36	3749	31
	4		9°		4,10	0,59	2,01	0,47	700	200	41	44	8
									1000	248	28	52	9
									2000	374	31	72	19
	5		24°		6,53	0,53	0,50	1,02	700	210	27	391	22
									1000	253	24	562	20
									2000	365	49	1138	40
	6		3°		9,63	0,49	0,49	0,96	700	240	16	269	17
									1000	286	22	379	20
									2000	402	50	738	42
					8,15	0,49	6,67	0,68	700	196	16	573	14
									1000	233	14	730	12
									2000	326	28	1168	24
9	1	HTO	13°	A	0,82	0,77	0,0034	1,67	300	66	31	46	8
									500	98	16	107	18
									1000	166	32	341	37
	2		54°		0,0025	1,79	0,78	0,79	300	70	17	72	16
									500	176	16	108	28
									1000	610	39	188	55
	3		19°		5,39	0,59	0,038	1,38	300	158	25	99	48
									500	213	34	200	39
									1000	321	75	520	69
					2,32	0,65	0,0043	1,68	300	96	18	63	8
									500	134	14	148	15
									1000	211	32	476	30
10	3	HTO	4°	B	0,0038	1,62	0,00051	1,90	500	90	7	69	23
									1000	276	8	259	9
									2000	850	19	969	18
	4		3°		0,35	0,91	0,0027	1,64	500	99	14	69	42
									1000	186	12	216	19
									2000	348	28	617	28
					0,048	1,21	0,0011	1,79	500	91	10	53	36
									1000	212	9	276	13
									2000	490	20	946	20

Table 1 Continued

Nr.	Period	Tracer	Δφ	Category	y σ_0	y p	z σ_0	z p	x [m]	σ_y [m]	$\frac{\Delta\sigma_y}{\sigma_y}$ [%]	σ_z [m]	$\frac{\Delta\sigma_z}{\sigma_z}$ [%]
11	1	HTO	5^o	C	4,30	0,43	0,0058	1,53	300	51	40	36	6
									700	73	14	130	14
									2000	116	37	648	31
	2		0^o		7,97	0,47	0,21	0,88	300	113	63	33	11
									700	168	24	70	19
									2000	274	44	177	39
	3		8^o		9,92	0,40	0,13	1,00	300	98	90	38	15
									700	137	24	90	34
									2000	209	96	257	65
	4		1^o		5,94	0,42	0,028	1,24	300	64	59	32	11
									700	79	31	92	26
									2000	140	57	336	54
	5		2^o		9,75	0,40	0,33	0,83	300	97	56	37	11
									700	136	23	57	17
									2000	208	39	179	50
					9,75	0,40	0,043	1,18	300	97	28	36	5
									700	136	10	97	13
									2000	209	28	333	26
13	1	HTO	8^o	D	3,48	0,47	1,30	0,81	700	88	9	268	9
									1500	107	11	499	7
									3000	147	20	877	13
	2		0^o		4,63	0,48	2,75	0,68	700	107	13	239	16
									1500	155	10	401	10
									3000	215	21	644	20
	3		9^o		7,13	0,45	4,86	0,58	700	135	15	223	16
									1500	191	13	349	11
									3000	260	25	522	21
					4,04	0,51	4,30	0,62	700	111	9	255	8
									1500	163	7	410	6
									3000	232	13	631	11
14	1	HTO	1^o	C	3,93	0,51	0,0031	1,53	500	91	16	42	5
									1000	129	8	120	10
									2000	183	20	346	20
	2		2^o		3,90	0,46	0,041	1,18	500	67	15	62	13
									1000	92	11	141	14
									2000	127	26	318	28
					3,89	0,48	0,0045	1,48	500	78	17	44	6
									1000	110	9	122	12
									2000	155	23	344	24

Table 1 Continued

Nr.	Period	Tracer	Δφ	Category	y		z		x	σ_y	$\frac{\Delta\sigma_y}{\sigma_y}$	σ_z	$\frac{\Delta\sigma_z}{\sigma_z}$
					σ_0	p	σ_0	p	[m]	[m]	[%]	[m]	[%]
14	1	CCl_4	0°	C	0,15	1,00	1,45	0,56	500	73	27	48	9
									1000	145	15	70	16
									2000	290	24	104	33
	2		1°		0,49	0,82	0,22	0,91	500	81	20	60	14
									1000	143	11	113	21
									2000	253	28	213	43
					0,035	1,22	1,24	0,61	500	70	19	53	8
									1000	163	10	81	17
									2000	280	19	123	35
15	1	HTO	4°	D	5,73	0,45	0,10	1,01	500	92	12	52	4
									1000	125	6	105	10
									2000	170	14	212	19
	2		1°		4,27	0,49	0,011	1,35	500	90	11	48	3
									1000	127	6	122	7
									2000	178	13	311	13
	3		6°		7,36	0,43	0,062	1,09	500	109	16	53	5
									1000	148	8	112	11
									2000	199	17	238	19
					7,00	0,43	0,036	1,17	500	98	8	51	2
									1000	132	4	115	5
									2000	177	9	258	10
15	1	CCl_4	3°	D	2,70	0,57	0,0070	1,44	500	93	16	54	6
									1000	138	11	145	13
									2000	205	23	394	24
	2		1°		0,76	0,76	0,0012	1,71	500	85	18	50	6
									1000	143	12	163	14
									2000	242	28	531	25
	3		7°		9,01	0,42	0,67	0,72	500	125	41	58	17
									1000	168	19	95	35
									2000	226	40	157	62
					1,67	0,66	0,028	1,22	500	103	14	53	5
									1000	163	8	124	11
									2000	258	19	287	20
17	1	HTO	0°	D	4,68	0,47	0,076	1,09	200	57	42	24	9
									500	88	14	66	10
									1000	122	20	141	21
	2		3°		4,16	0,53	0,15	0,99	200	67	42	28	8
									500	108	13	70	12
									1000	156	25	138	23

Table 1 Continued

Nr.	Period	Tracer	Δφ	Category	y σ_0	y p	z σ_0	z p	x [m]	σ_y [m]	$\Delta\sigma_y/\sigma_y$ [%]	σ_z [m]	$\Delta\sigma_z/\sigma_z$ [%]
17	3	HTO	1^0	D	2,95	0,56	0,22	0,90	200	56	32	26	6
									500	94	12	59	6
									1000	138	17	110	13
					7,20	0,41	0,113	1,02	200	63	20	25	4
									500	92	7	63	4
									900	118	9	115	8
18	2	HTO	43^0	B	0,0038	1,80	1,78	0,55	200	54	58	33	21
									500	284	30	54	11
									1000	993	23	79	28
	3		53^0		0,0009	1,97	0,059	1,11	200	32	88	21	28
									500	193	32	57	16
									1000	759	28	123	42
					0,0018	1,92	0,016	1,34	200	33	54	25	16
									500	202	25	52	8
									1000	797	15	91	21
18	2	CCl_4	49^0	B	0,44	1,05	1,41	0,59	200	114	45	32	14
									500	298	22	55	9
									1000	617	14	83	20
	3		49^0		2,37	0,81	6,89	0,47	200	173	47	81	114
									500	364	24	124	62
									1000	638	42	172	53
					0,26	1,13	1,28	0,63	200	106	40	35	16
									500	300	18	62	11
									1000	657	14	96	26
19	2	HTO	50^0	A	0,36	1,09	0,88	1,04	100	55	34	104	45
									500	317	55	555	49
									1500	1049	104	1735	96
19	2	CCl_4	43^0	A	0,31	0,99	0,36	1,15	100	30	35	70	67
									500	147	42	445	37
									1500	438	83	1568	86
20	1	CCl_4	2^0	B	2,49	0,73	0,0039	1,64	300	160	27	44	6
									600	265	14	138	19
									1600	543	46	688	40
23	3	HTO	4^0	E	0,78	0,91	0,67	0,59	500	223	154	26	16
									1400	568	78	47	19
									3900	1441	40	85	34
23	3	$CFCl_3$	6^0	E	6,88	0,56	0,78	0,63	500	222	94	39	16
									1400	394	33	75	35
									3900	699	48	143	64

Table 1 Continued

Nr.	Period	Tracer	$\Delta\varphi$	Category	y σ_0	y p	z σ_0	z p	x [m]	σ_y [m]	$\frac{\Delta\sigma_y}{\sigma_y}$ [%]	σ_z [m]	$\frac{\Delta\sigma_z}{\sigma_z}$ [%]
24	1	HTO	3^0	D	0,33	0,82	0,11	0,98	400	44	91	38	15
									700	69	48	66	24
									1500	128	43	139	52
	2		2^0		0,82	0,77	0,11	0,99	400	81	35	42	7
									700	124	17	73	12
									1500	222	21	154	21
					3,66	0,51	0,082	1,05	400	75	38	43	7
									700	100	19	76	13
									1500	147	29	168	23
24	1	CBr_2F_2	5^0	D	2,61	0,52	0,056	1,11	400	57	37	44	9
									700	77	18	83	16
									1500	114	28	193	30
	2		6^0		0,042	1,16	0,036	1,18	400	44	19	42	5
									700	95	10	80	7
									1500	206	14	197	13
					0,277	0,86	0,023	1,26	400	48	20	42	5
									700	78	10	85	8
									1500	157	15	220	14
25	1	HTO	2^0	D	0,0605	1,11	0,19	0,88	400	47	34	37	6
									800	102	15	68	11
									2000	281	24	152	30
25	1	CBr_2F_2	4^0	D	0,11	1,09	0,15	0,89	400	74	37	31	7
									800	158	18	57	9
									2000	427	20	129	24

Table 2 Mean Dispersion Parameters

Nr.	Period	TRACER	Category	y		z		x	σ_y	$\frac{\Delta \sigma_y}{\sigma_y}$	σ_z	$\frac{\Delta \sigma_z}{\sigma_z}$
				σ_0	p	σ_0	p	[m]	[m]	[%]	[m]	[%]
10	3	HTO	B	0,16	1,08	0,0005	1,91	200	50	32	14	12
	4							600	164	9	108	8
18	2							1200	348	19	418	17
	3							2000	605	32	1112	24
11	1	HTO	C	9,03	0,42	0,044	1,17	200	83	31	22	7
	2							600	132	9	78	8
	3							1200	176	11	177	13
	4							2000	218	21	320	18
	5											
14	1											
	2											
15	1	HTO	D	2,97	0,56	0,19	0,92	200	56	18	24	5
	2							600	103	7	65	4
	3							1200	152	6	122	7
								2000	201	10	194	11
17	1											
	2											
	3											
24	1											
	2											
25	1											
15	1	CCl_4	D	0,69	0,78	0,024	1,23	200	43	28	16	10
	2							600	100	10	62	4
	3							1200	172	8	145	9
								2000	256	15	270	15
24	1	CBr_2F_2										
	2											
25	1	CBr_2F_2										

Table 3 Results of Experiment 15 for the Reflection and Total Absorption Model

Period	Reflection					Total Absorption				
	$R \cdot 10^8$ (m^{-2})	σ_{oy}	p_y	σ_{oz}	p_z	$R \cdot 10^8$ (m^{-2})	σ_{oy}	p_y	σ_{oz}	p_z
1	182	5,73	0,45	0,10	1,01	166	5,81	0,42	1,47	0,57
2	150	4,27	0,49	0,011	1,35	161	1,54	0,61	0,24	0,84
3	204	7,36	0,43	0,062	1,09	230	5,46	0,45	0,84	0,66
combined	211	7,00	0,43	0,036	1,17	210	6,54	0,41	0,58	0,71

Table 4 Assignment of our σ_z curves to those by Pasquill and Gifford

Meteorologically defined category according to Pasquill	Sequential number of experiment	Assigned σ_z curve according to Pasquill/Gifford
A	9 (HTO)	A
A	19 (HTO)	> A
A	19 (CCl_4)	> A
B	10 (HTO)	A/B
B	18 (HTO)	B
B	18 (CCl_4)	B_f
B	20 (CCl_4)	A/B
C	3 (HTO)	C_s
C	6 (HTO)	C
C	11 (HTO)	B
C	14 (HTO)	B
C	14 (CCl_4)	B/C_f
D	1 (HTO)	D
D	7 (HTO)	C_s
D	13 (HTO)	A/B_f
D	15 (HTO)	B
D	15 (CCl_4)	B
D	17 (HTO)	A/B
D	24 (HTO)	B
D	24 (CBr_2F_2)	B
D	25 (HTO)	B/C_f
D	25 (CBr_2F_2)	C
E	23 (HTO)	C/D
E	23 ($CFCl_3$)	C/D

The abbreviations have the following meanings explained by the examples below:

A/B: between categories A and B

C_s: curve has a steeper slope than the Pasquill/Gifford curve of category C

C_f: curve has a flatter slope than the Pasquill/Gifford curve of category C

Table 5 Assignment of the σ_z curves calculated for the different categories to the σ_z curves according to Pasquill/Gifford

Meteorologically defined category according to Pasquill	Corresponding σ_z curve from the family of σ_z curves according to Pasquill/Gifford
A	>A
B	A/B
C	B
D_T (D during the daytime)	B
E	C/D

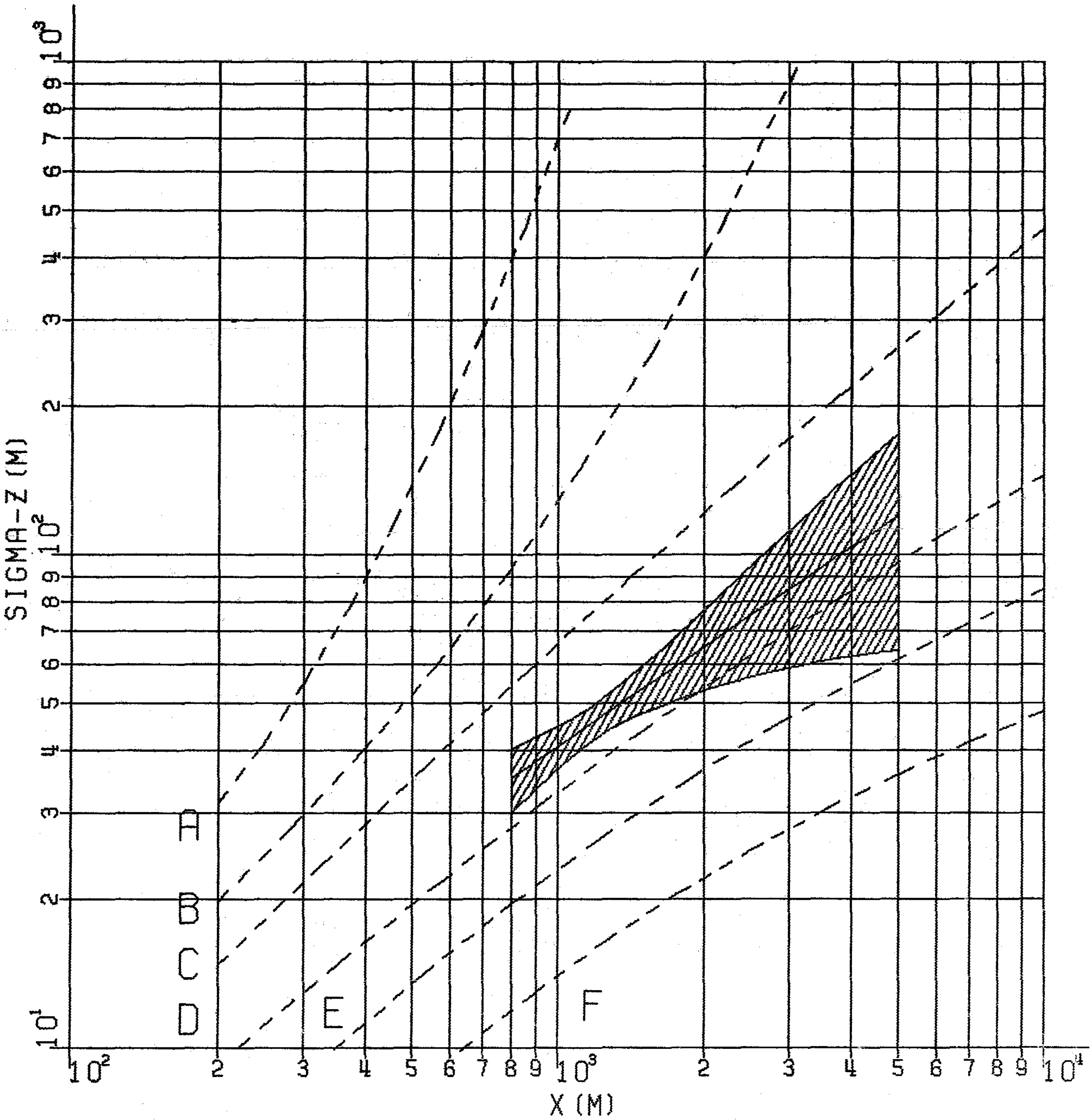

Fig. 1 : Vertical Dispersion Parameter of Experiment 1 (HTO), Period 1
(--- Pasquill-Gifford)

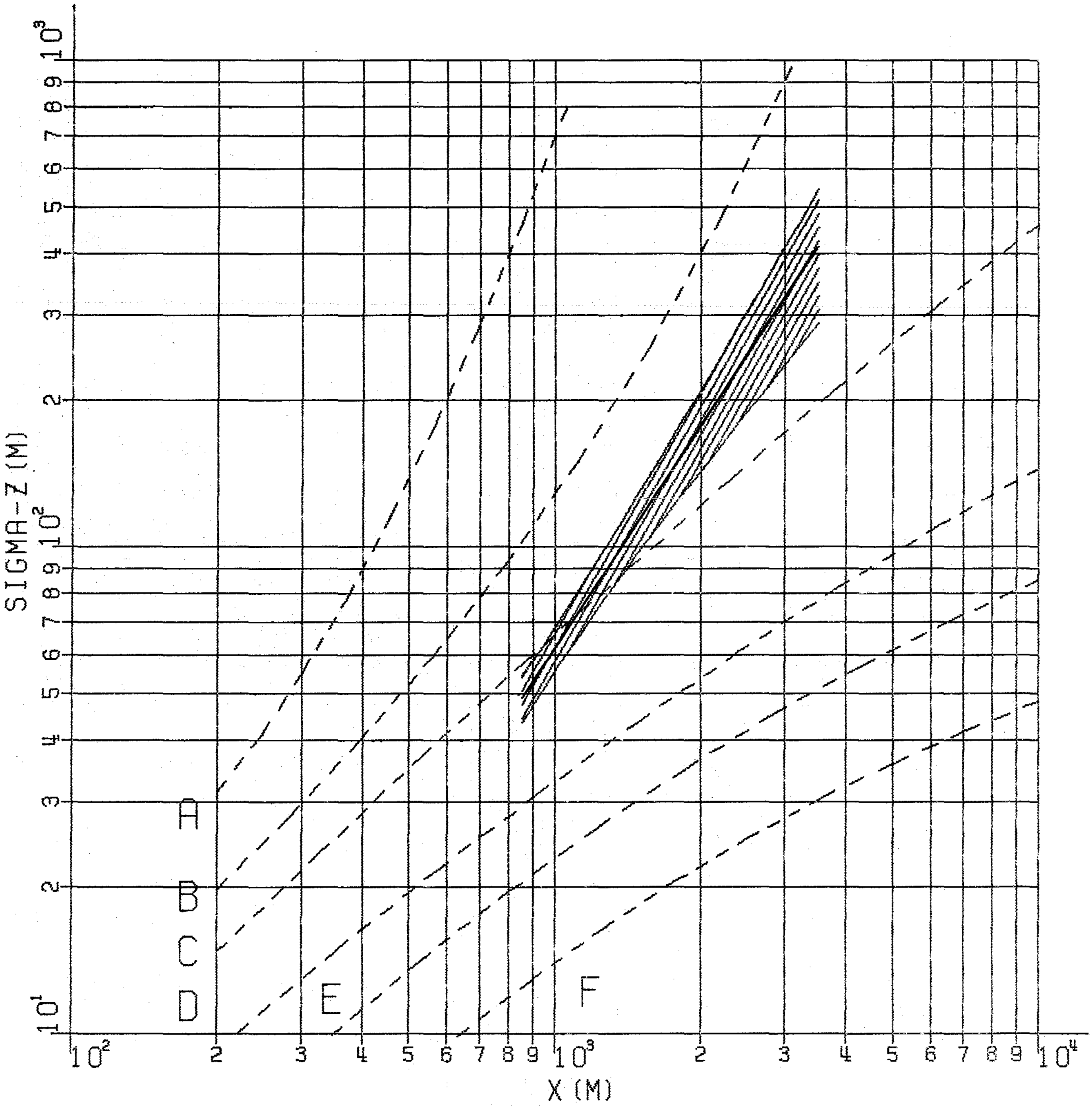

Fig. 2 : Vertical Dispersion Parameter of Experiment 3 (HTO), Periods 2, 3
(--- Pasquill-Gifford)

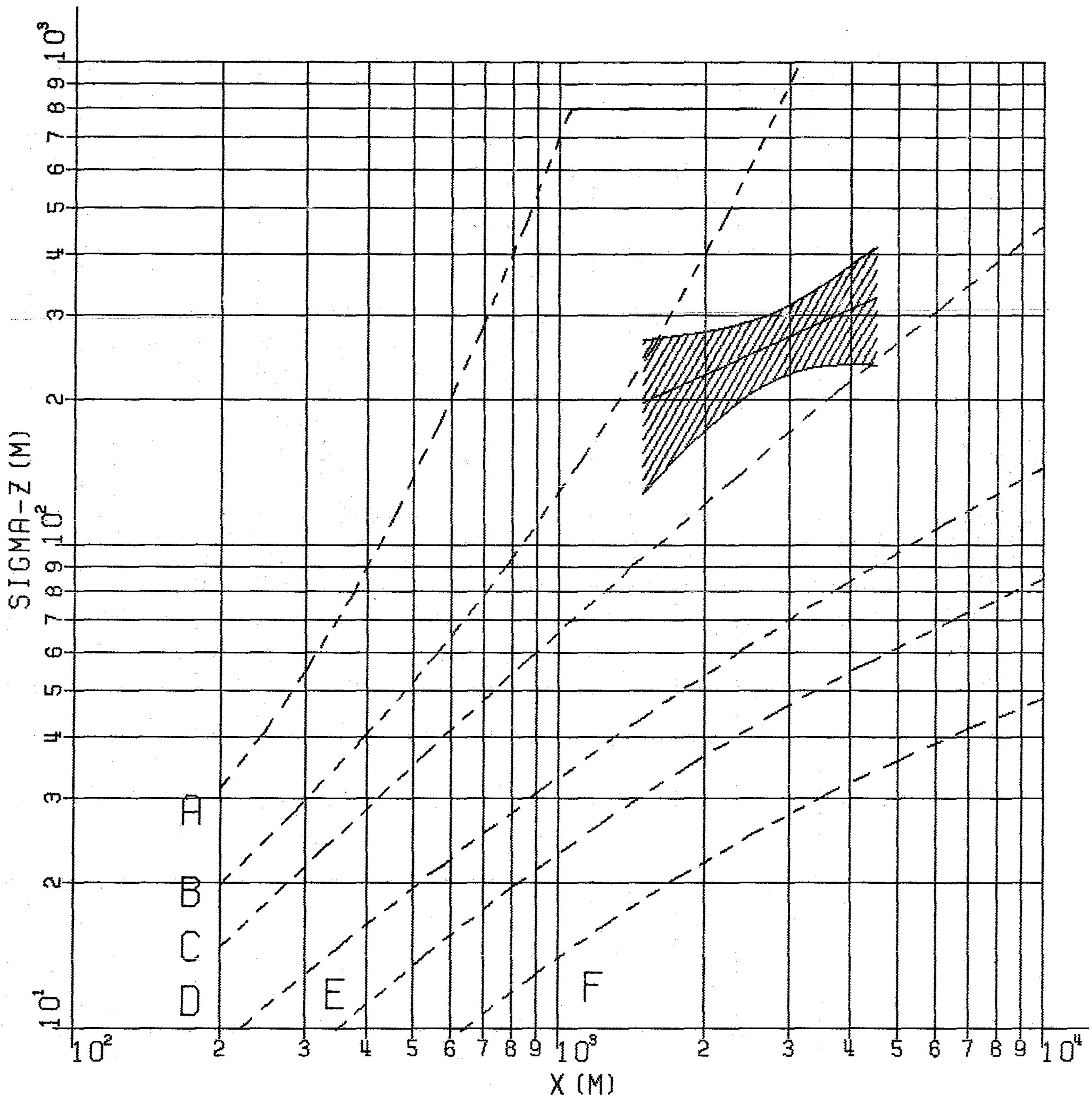

Fig. 3 : Vertical Dispersion Parameter of Experiment 6 (HTO), Periods 1, 2, 3, 4, 5, 6 (--- Pasquill-Gifford)

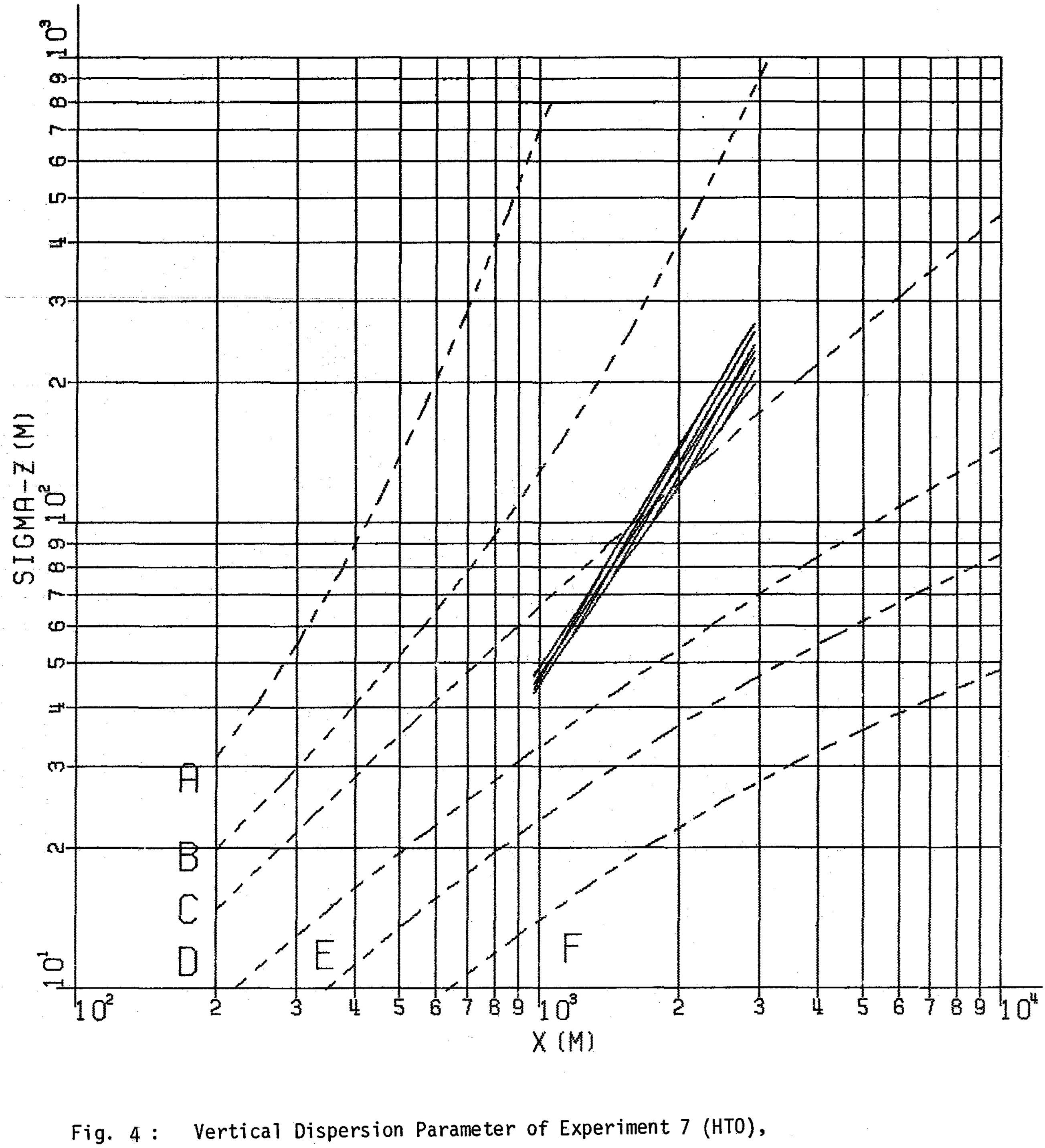

Fig. 4 : Vertical Dispersion Parameter of Experiment 7 (HTO),
Periods 2, 3, 4, 5
(--- Pasquill-Gifford)

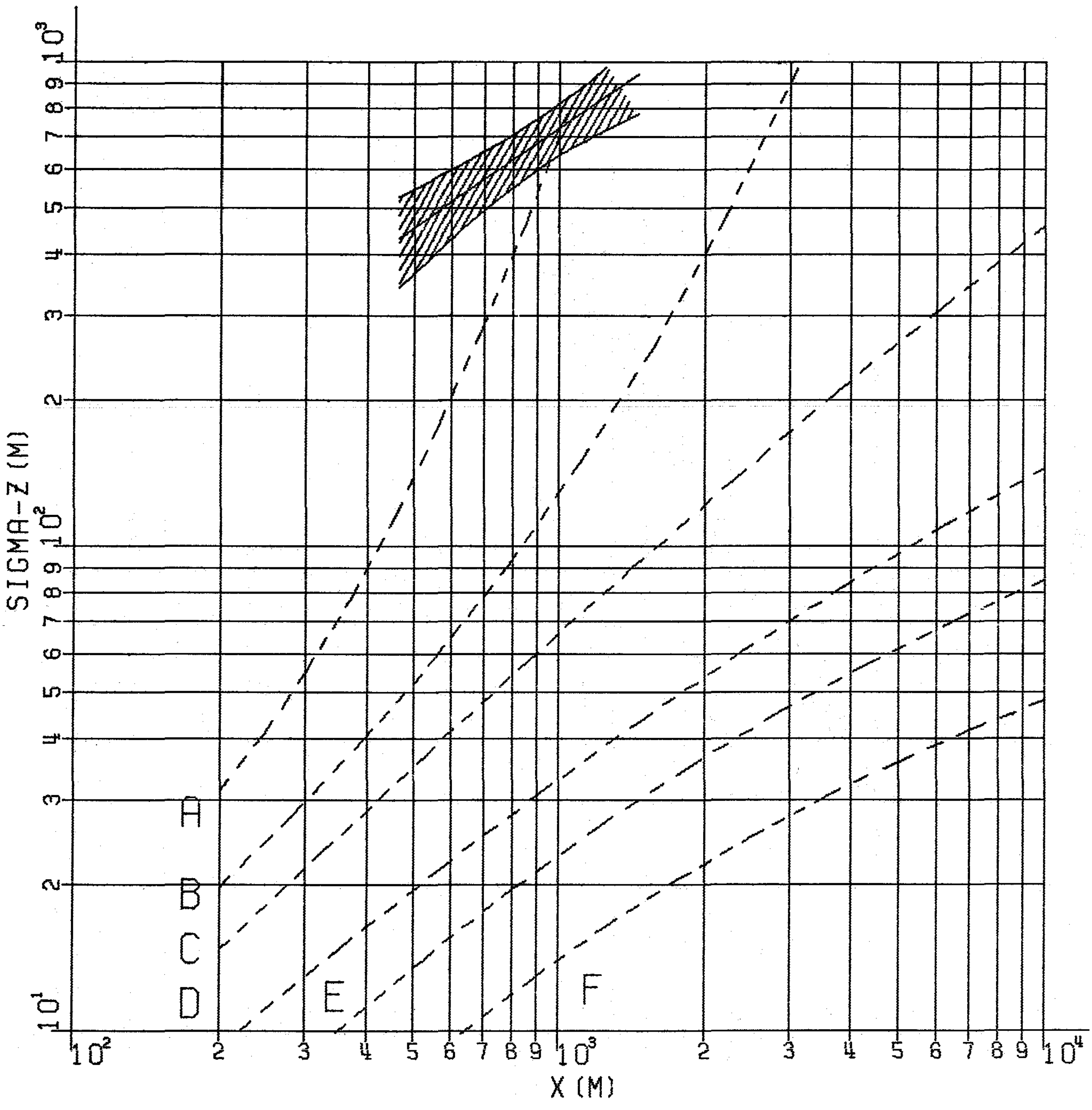

Fig. 5 : Vertical Dispersion Parameter of Experiment 8 (HTO), Periods 3, 4, 5, 6
(--- Pasquill-Gifford)

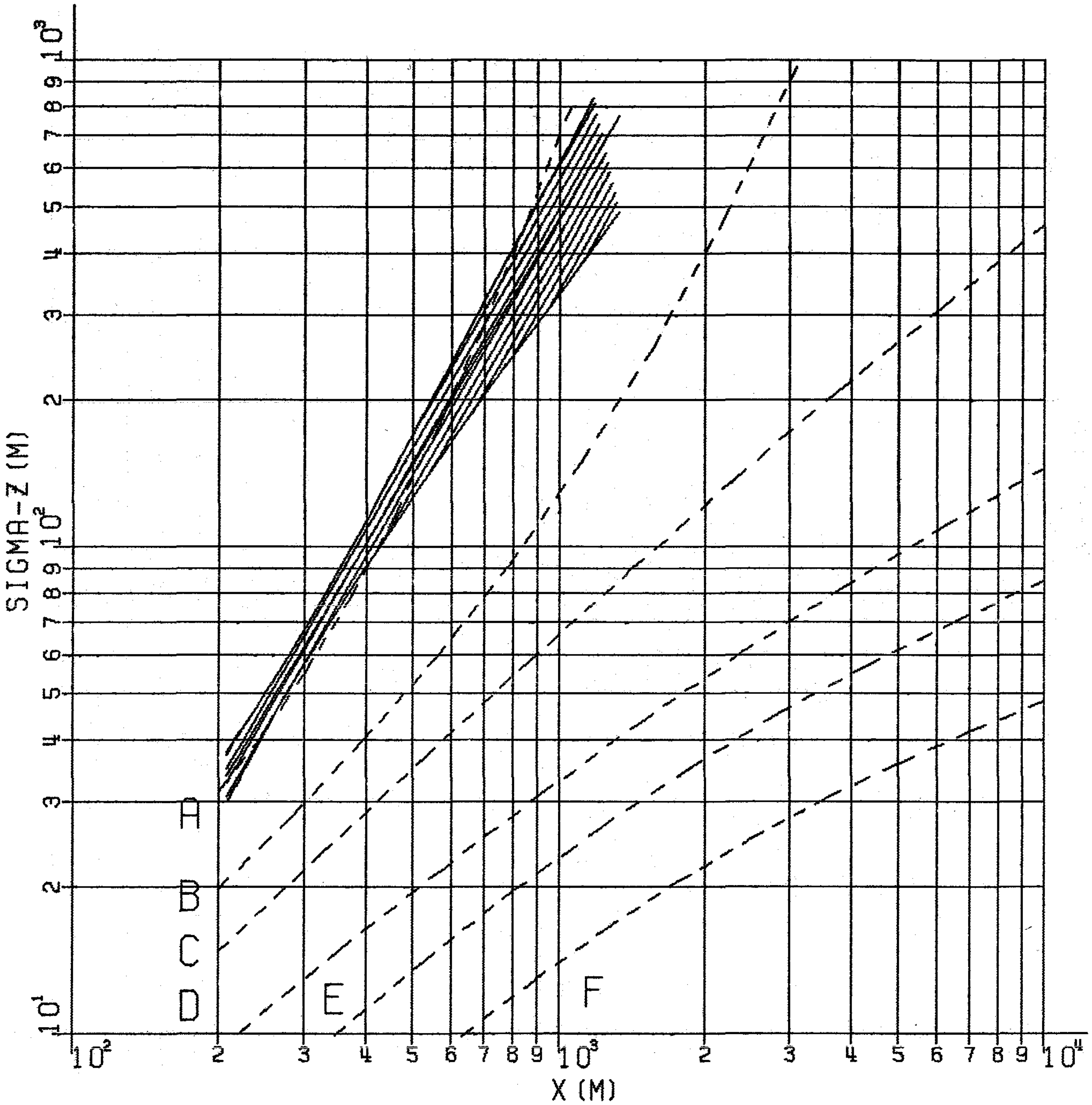

Fig. 6 : Vertical Dispersion Parameter of Experiment 9 (HTO), Periods 1, 2, 3
(--- Pasquill-Gifford)

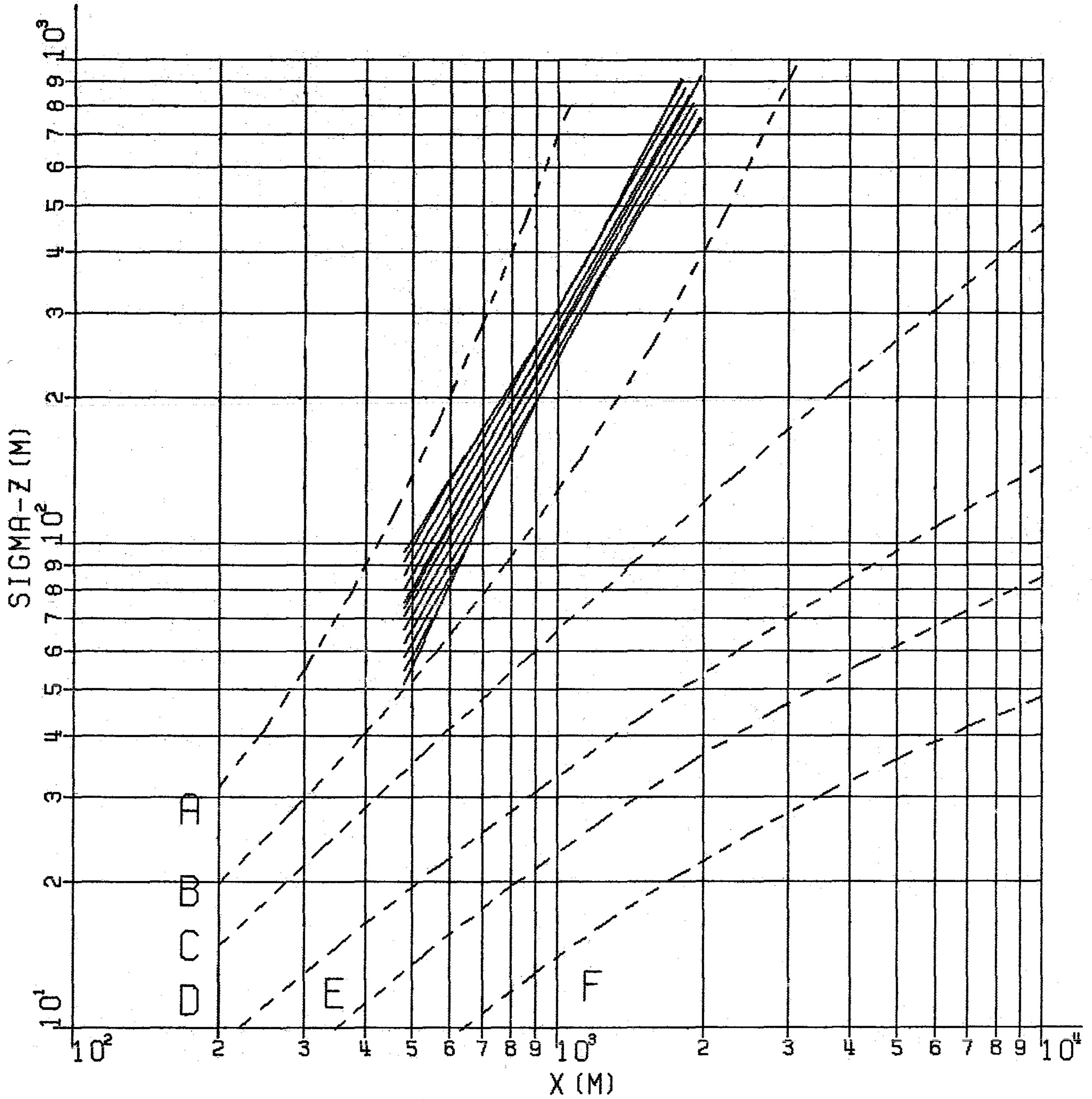

Fig. 7 : Vertical Dispersion Parameter of Experiment 10 (HTO), Periods 3, 4
(--- Pasquill-Gifford)

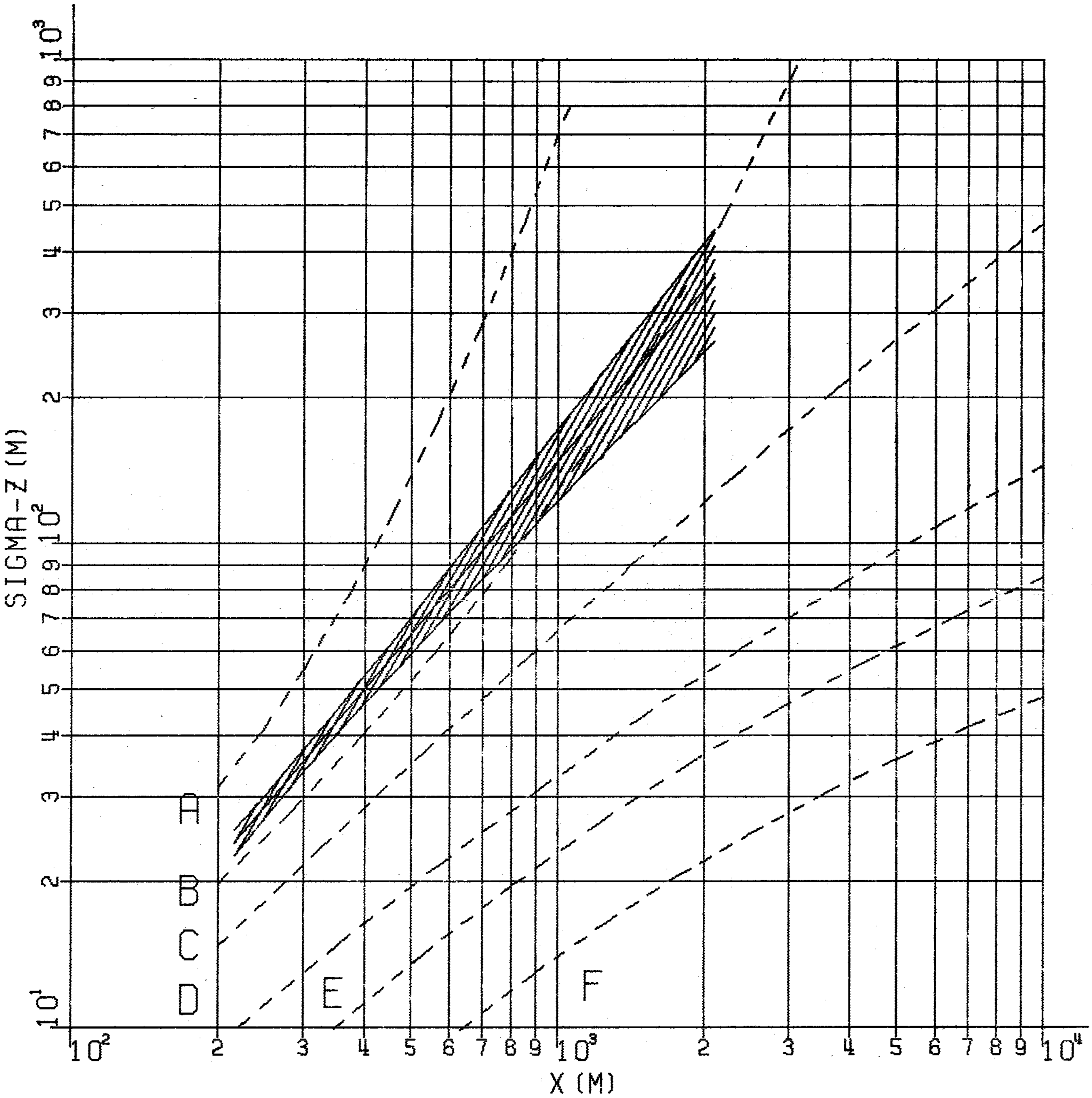

Fig. 8 : Vertical Dispersion Parameter of Experiment 11 (HTO), Periods 1, 2, 3, 4, 5
(--- Pasquill-Gifford)

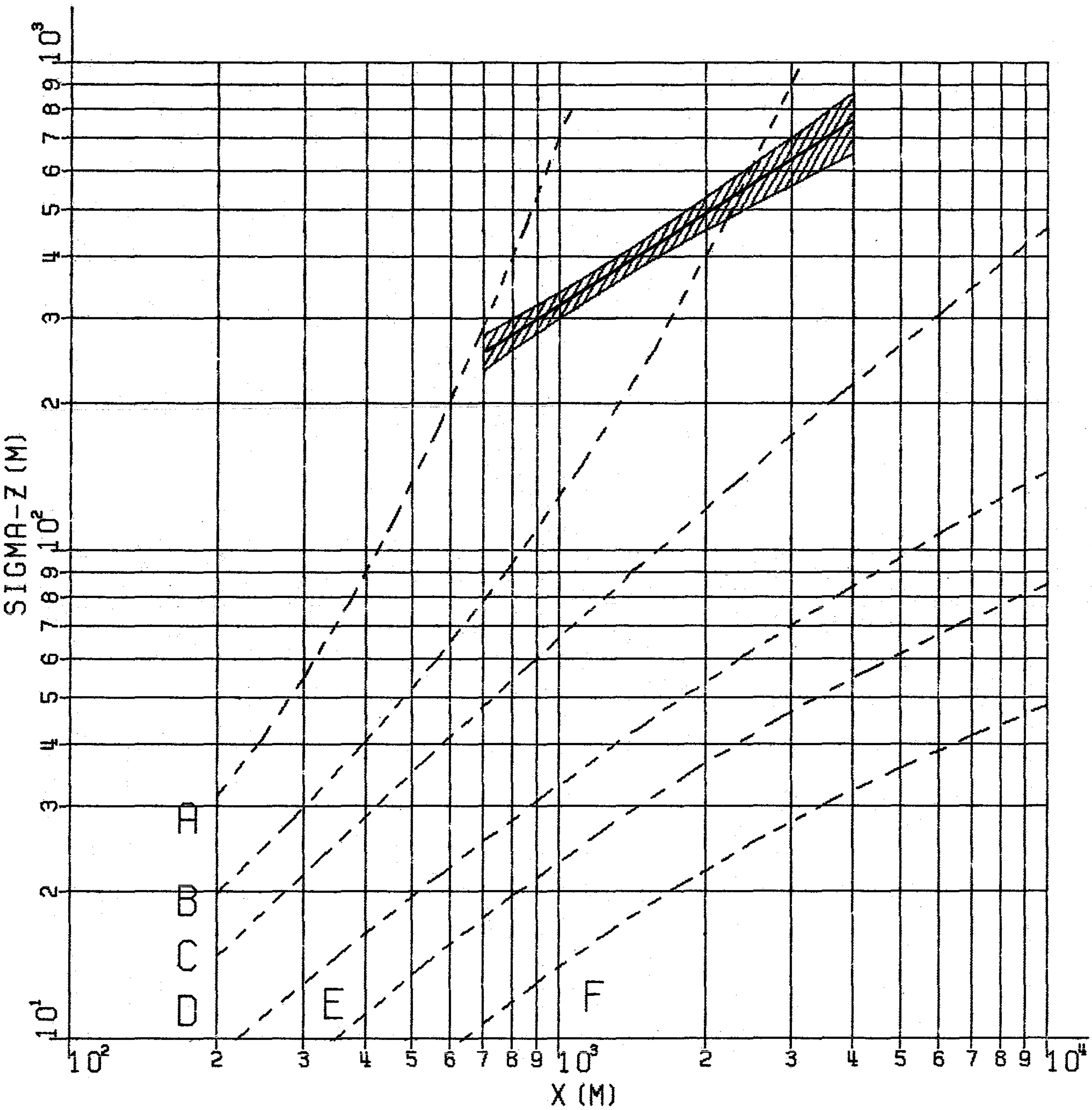

Fig. 9 : Vertical Dispersion Parameter of Experiment 13 (HTO), Periods 1, 2, 3
(--- Pasquill-Gifford)

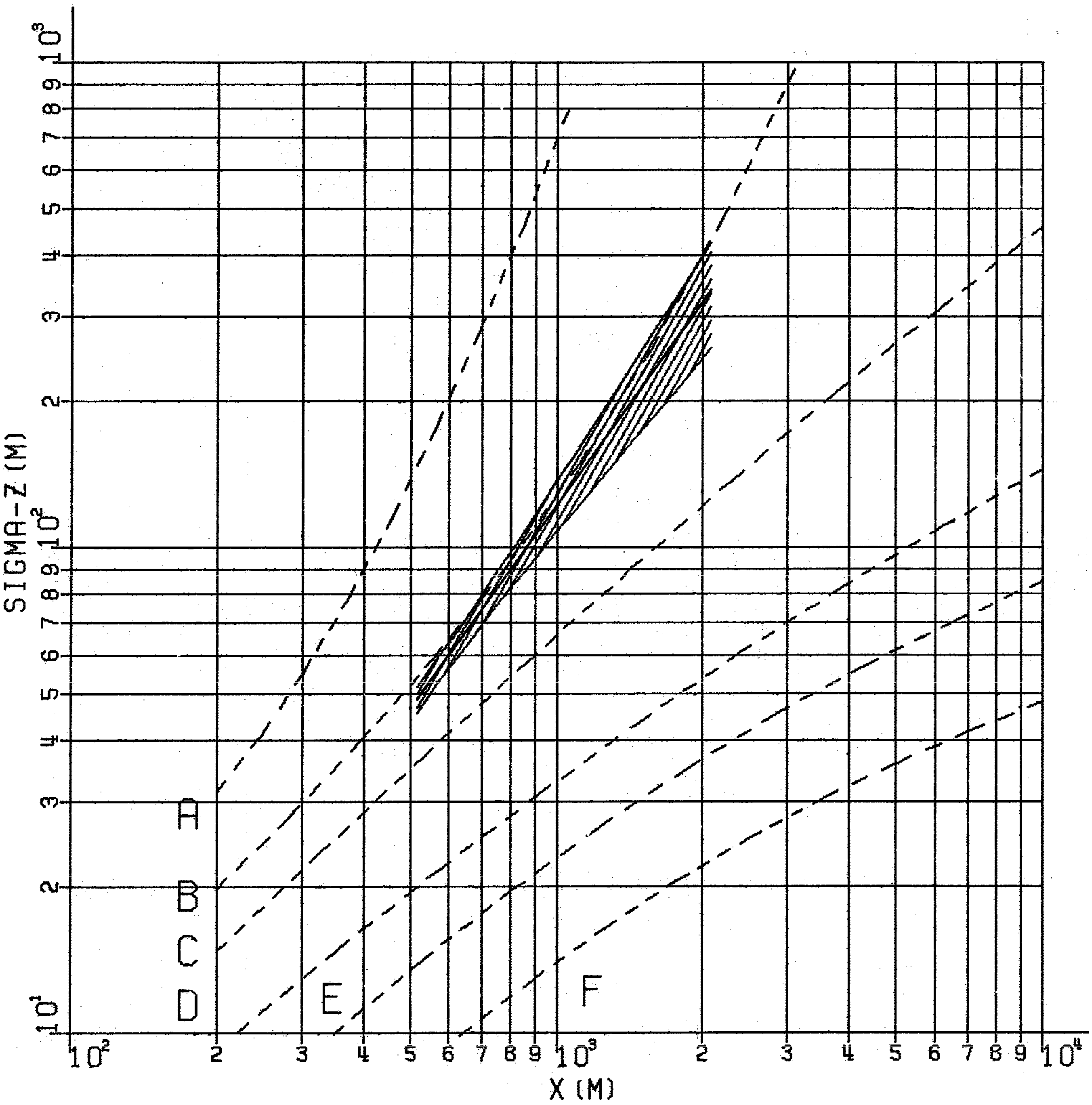

Fig. 10 : Vertical Dispersion Parameter of Experiment 14 (HTO),
Periods 1, 2
(--- Pasquill-Gifford)

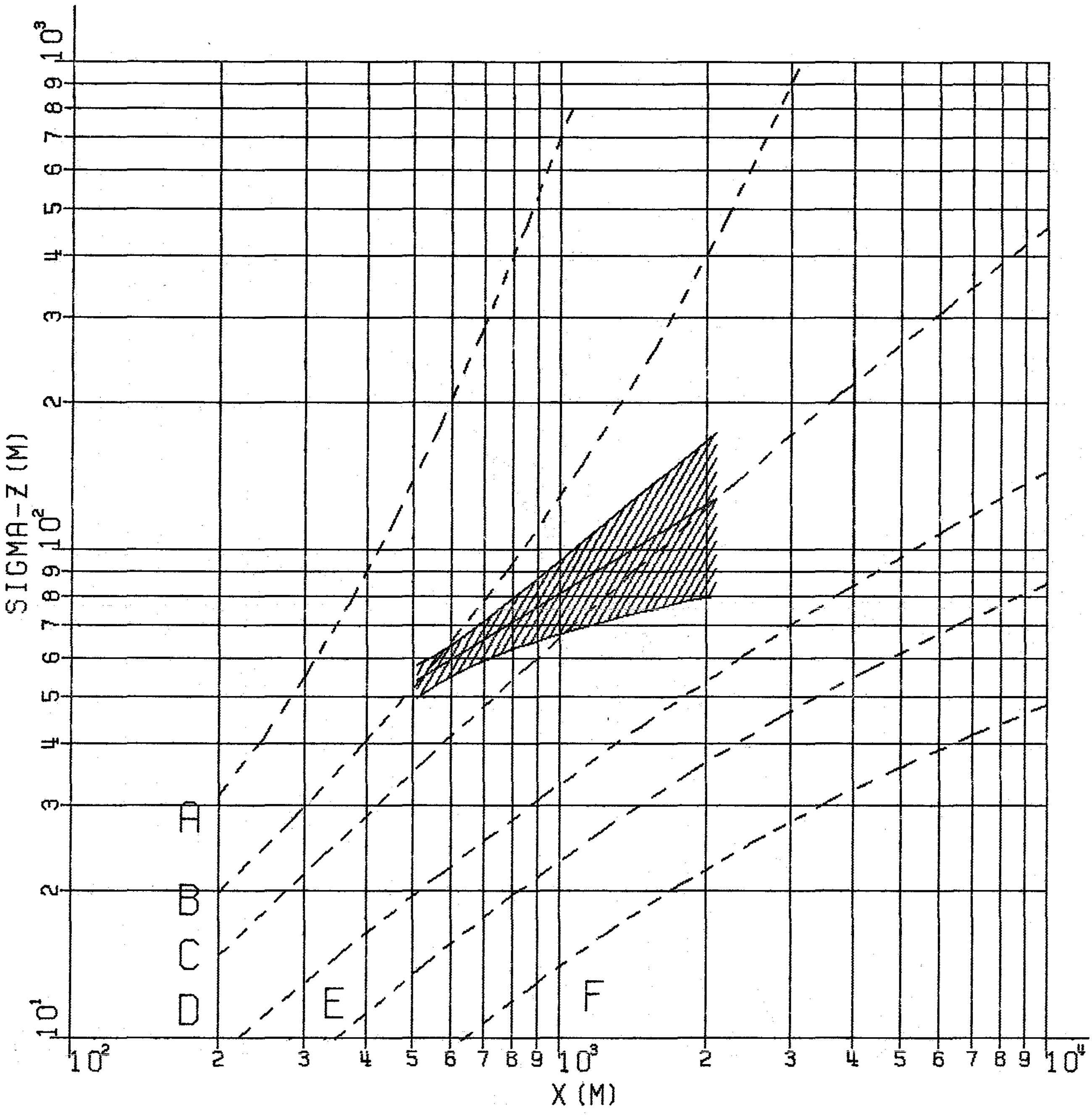

Fig. 11: Vertical Dispersion Parameter of Experiment 14 (CCl_4), Periods 1, 2
(--- Pasquill-Gifford)

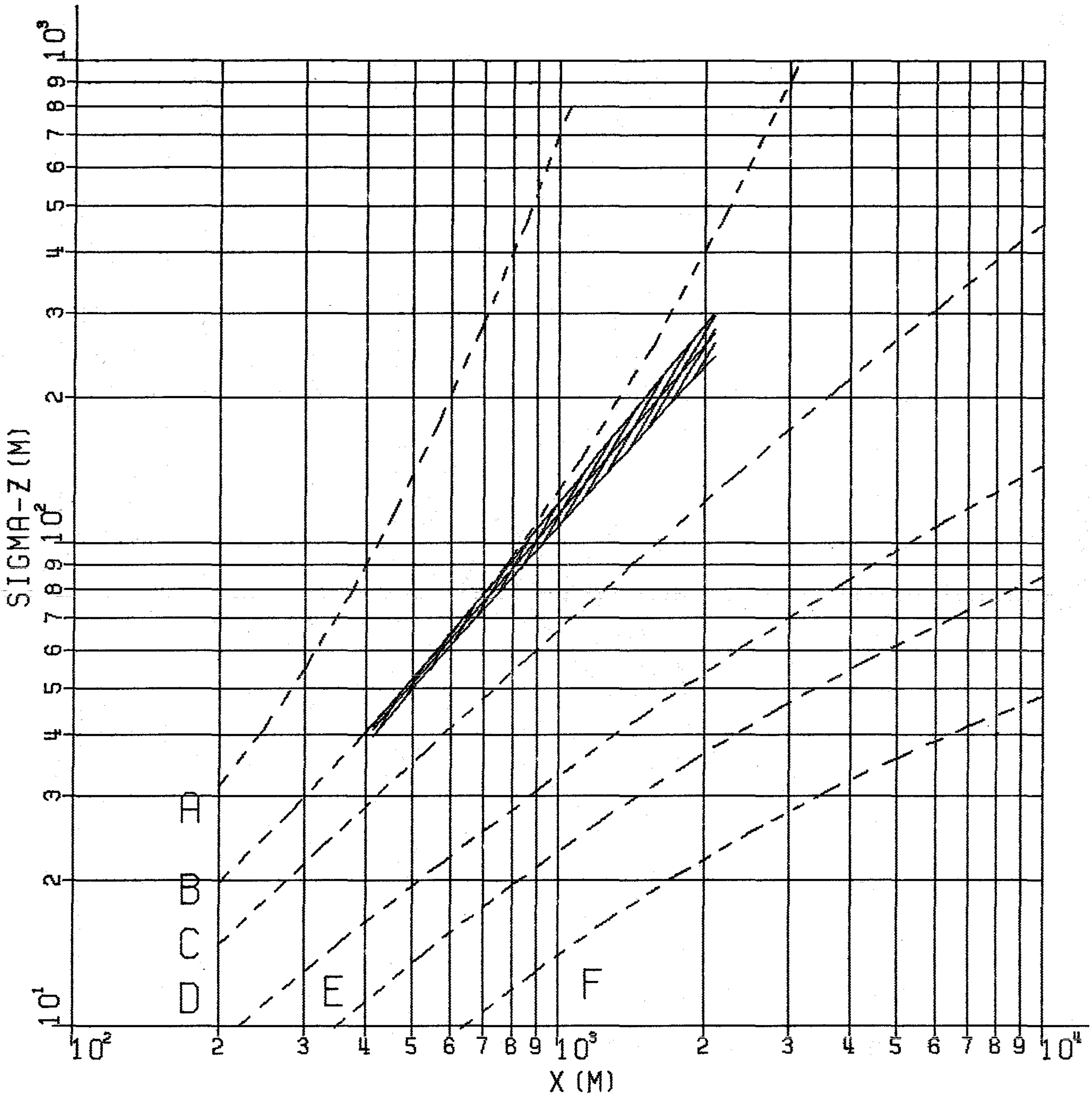

Fig. 12: Vertical Dispersion Parameter of Experiment 15 (HTO),
Periods 1, 2, 3
(--- Pasquill-Gifford)

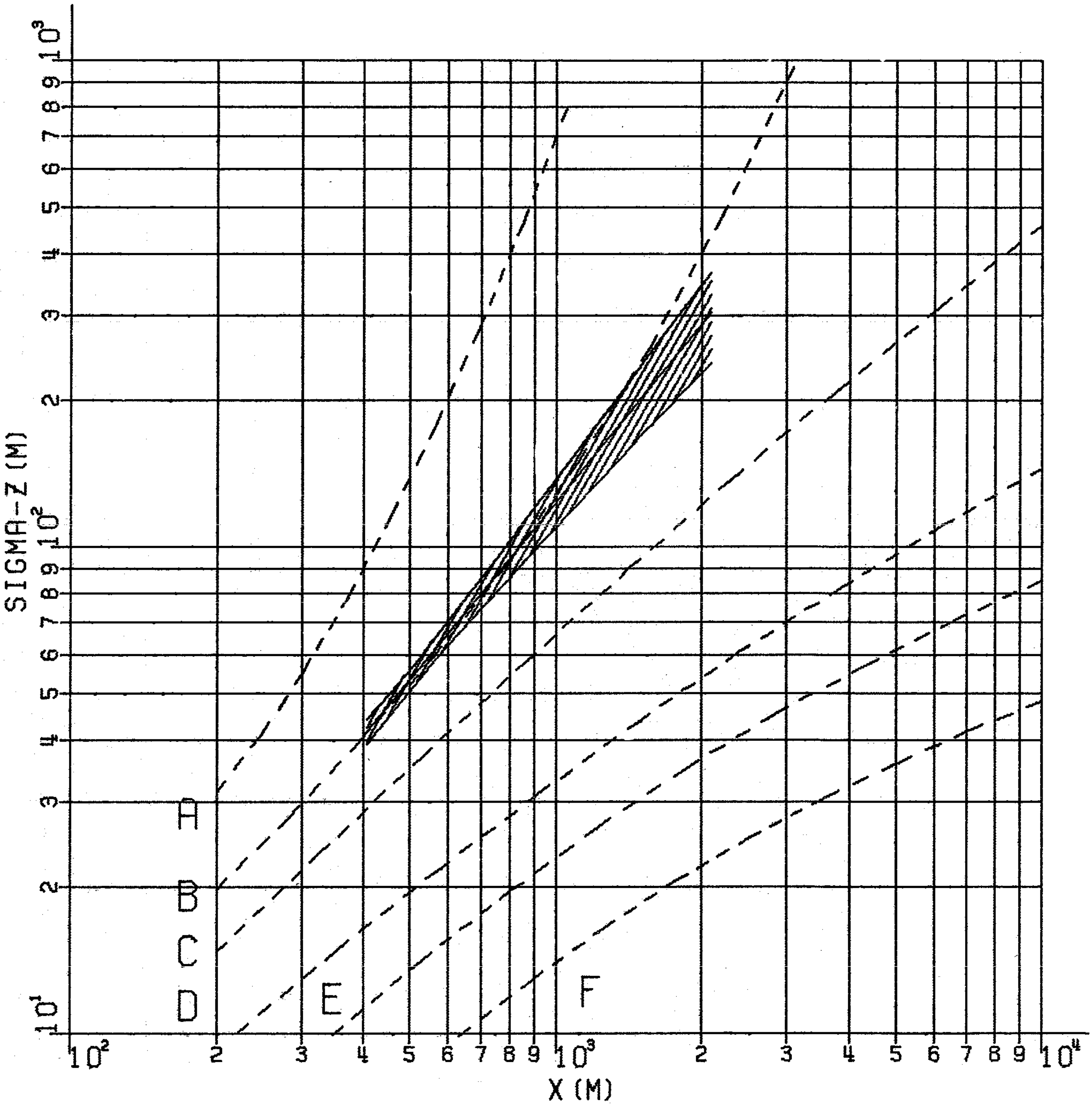

Fig. 13: Vertical Dispersion Parameter of Experiment 15 (CCl_4), Periods 1, 2, 3
(--- Pasquill-Gifford)

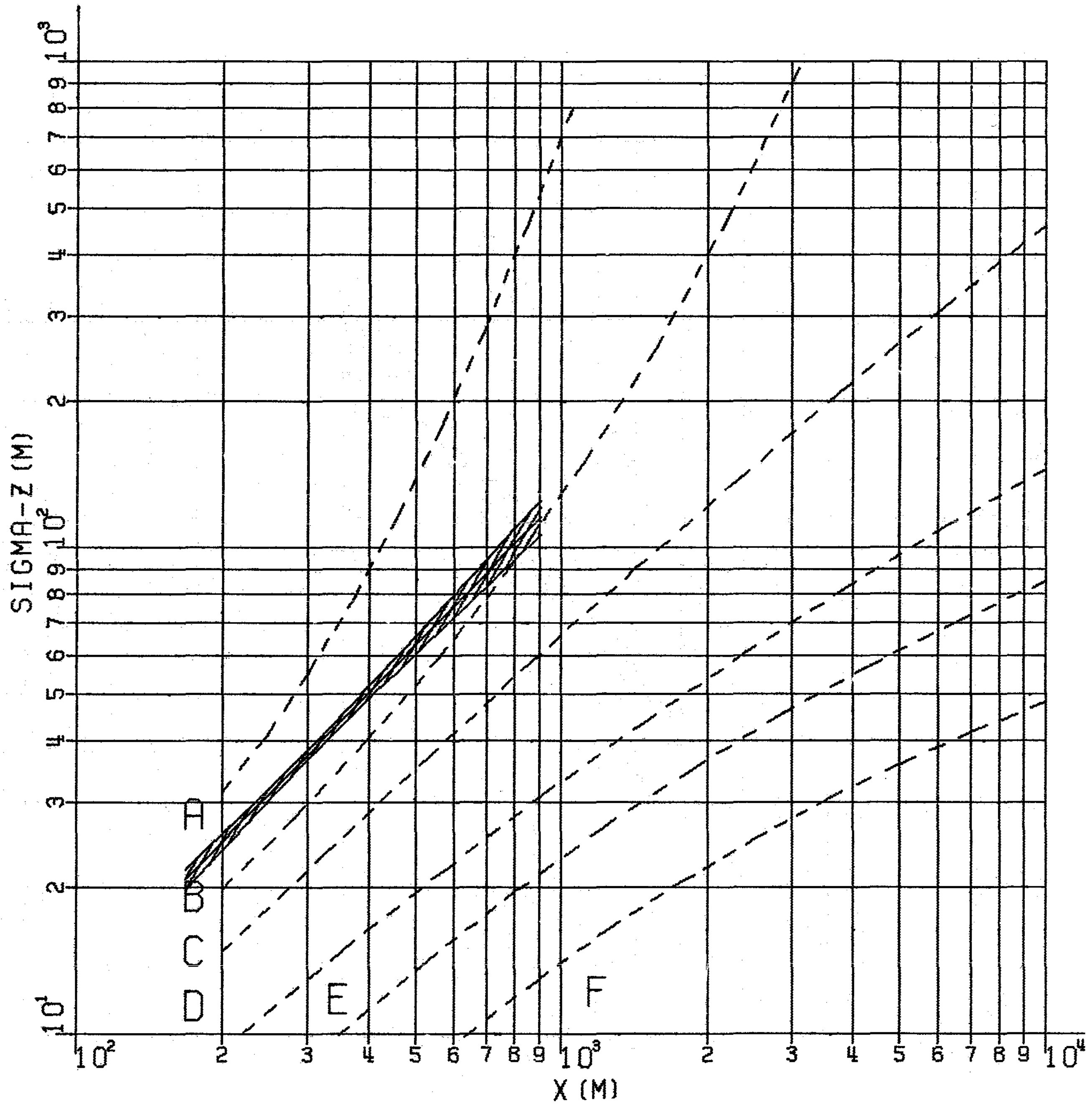

Fig. 14: Vertical Dispersion Parameter of Experiment 17 (HTO), Periods 1, 2, 3
(--- Pasquill-Gifford)

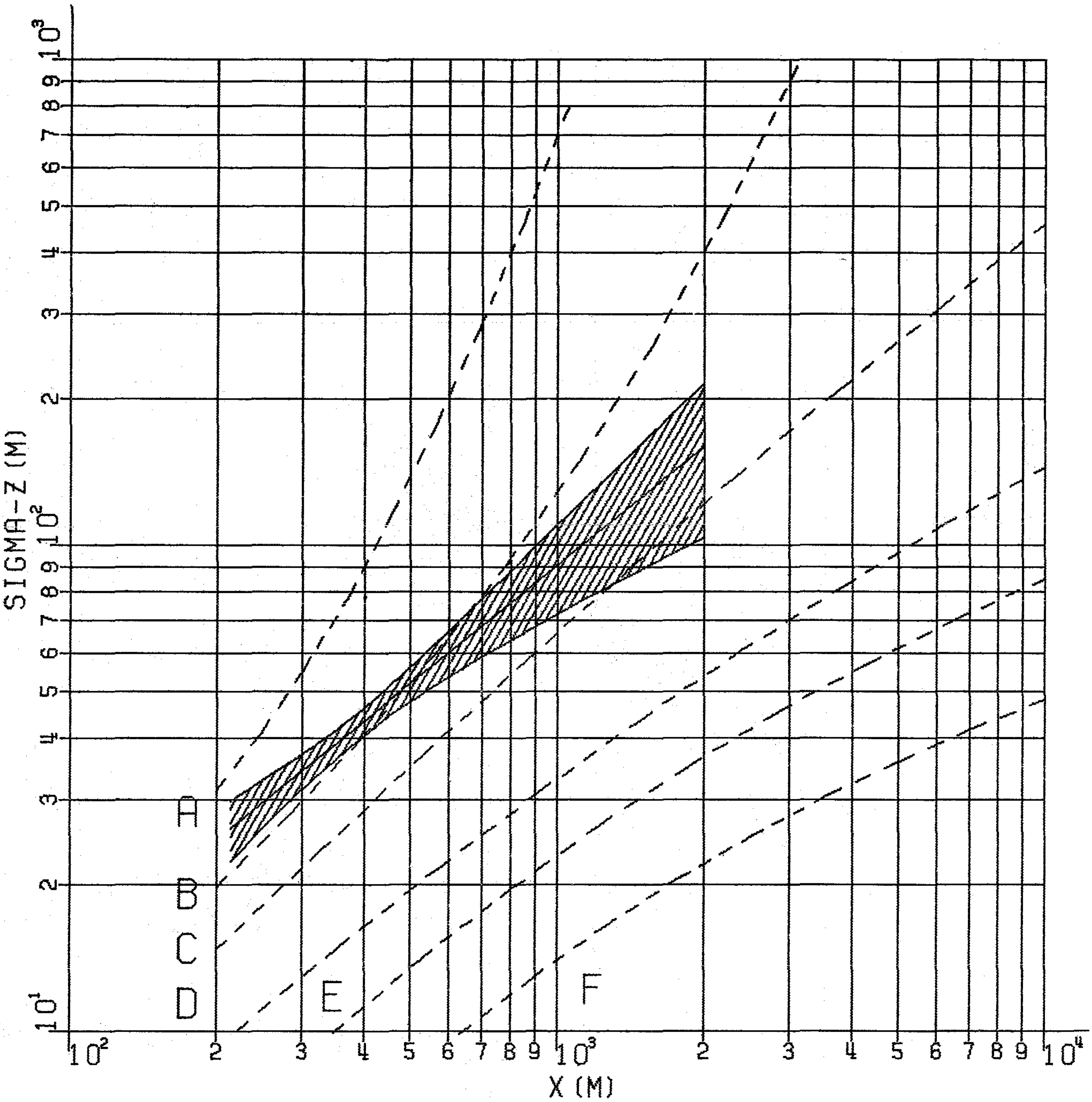

Fig. 15: Vertical Dispersion Parameter of Experiment 18 (HTO), Periods 2, 3
(--- Pasquill-Gifford)

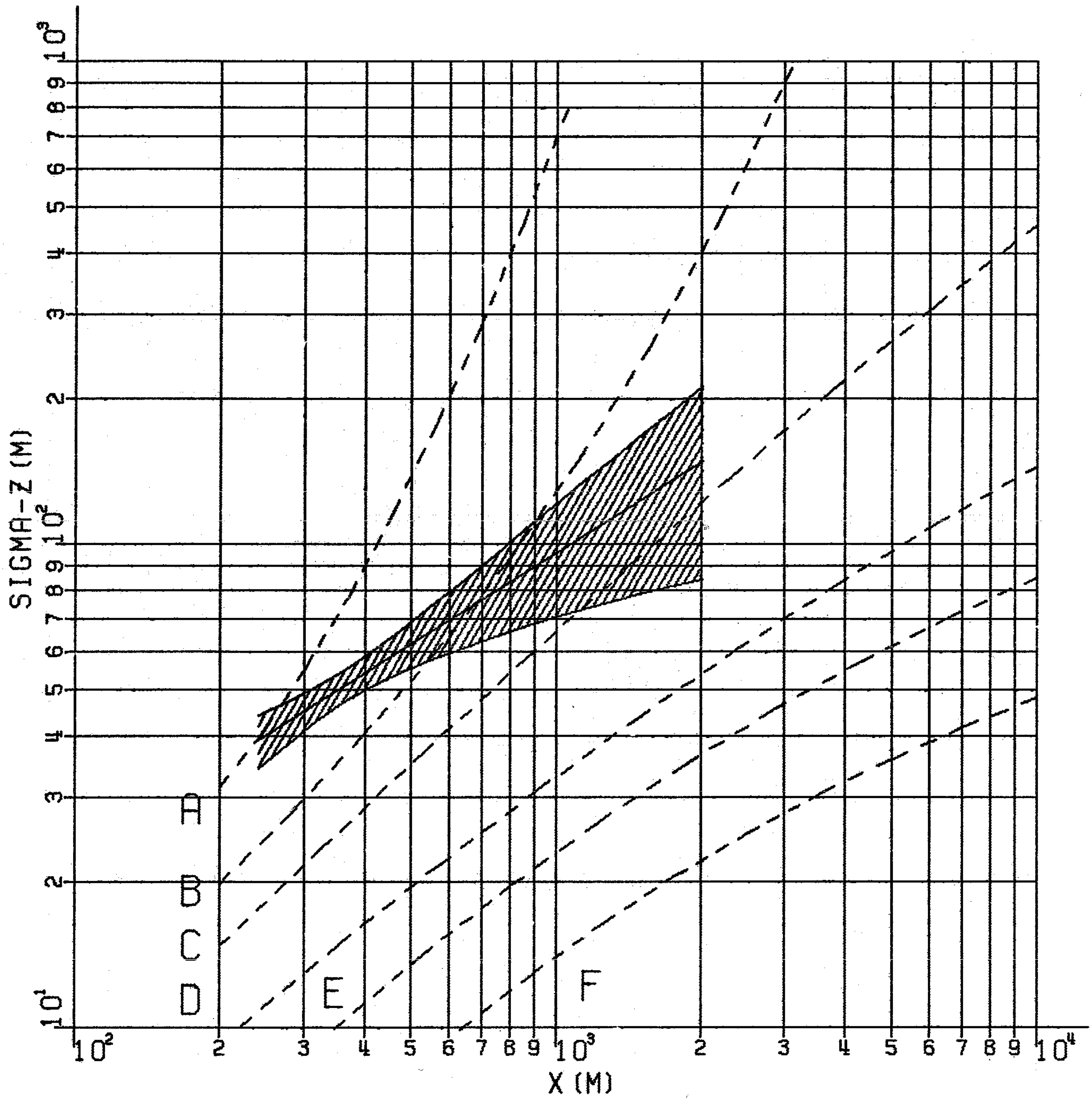

Fig. 16: Vertical Dispersion Parameter of Experiment 18 (CCl_4), Periods 2, 3
(--- Pasquill-Gifford)

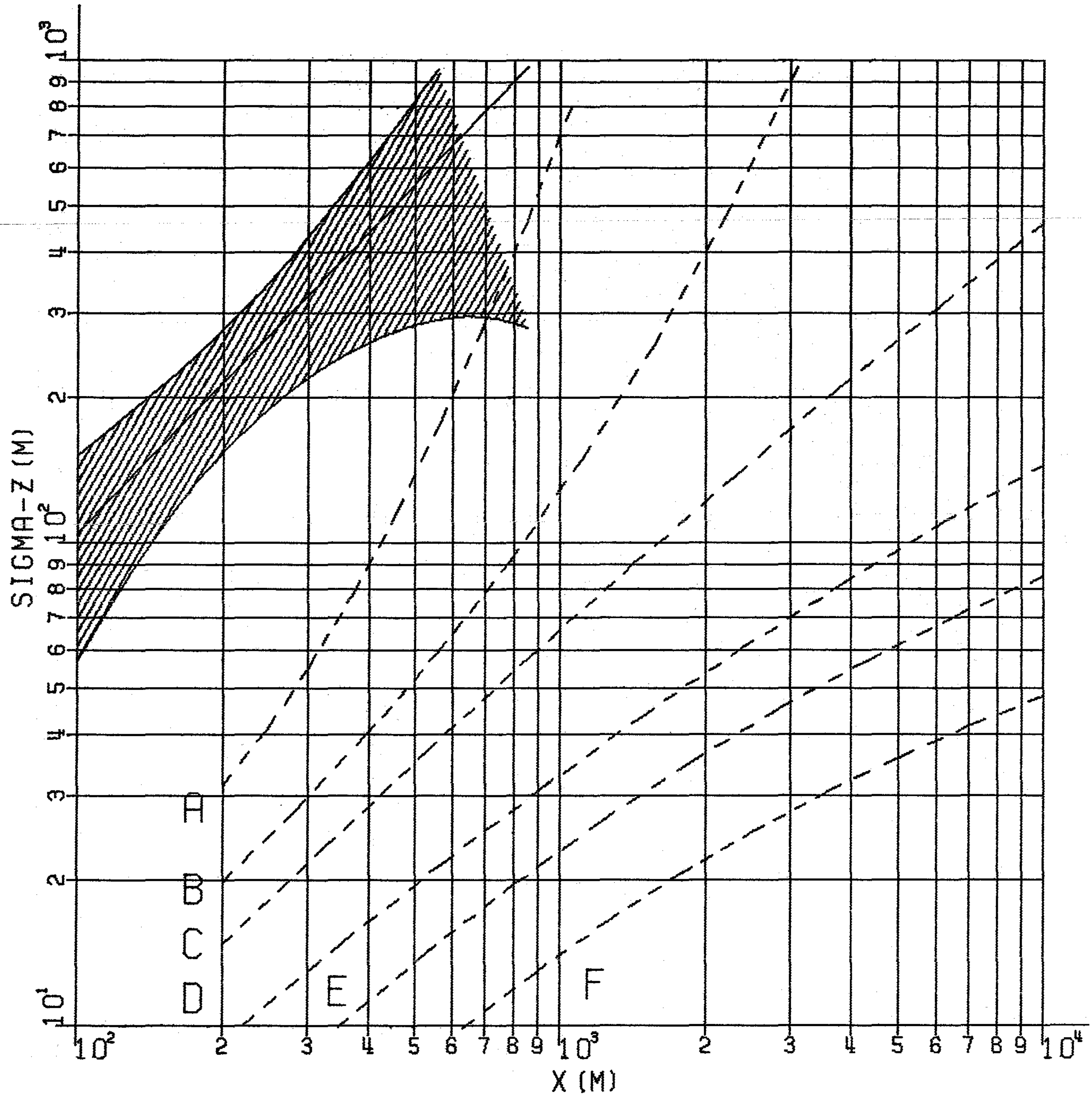

Fig. 17: Vertical Dispersion Parameter of Experiment 19 (HTO), Period 2 (--- Pasquill-Gifford)

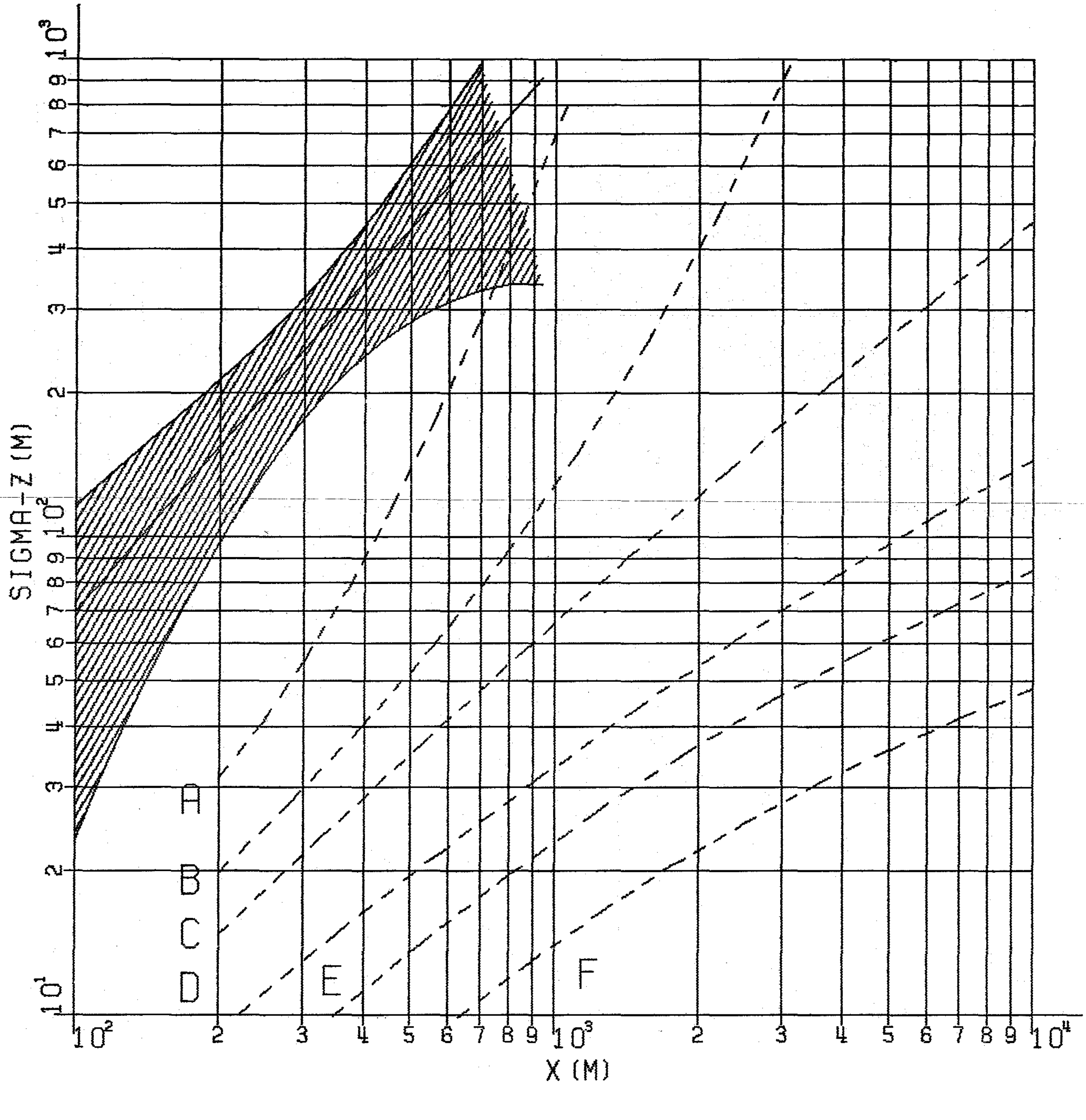

Fig. 18: Vertical Dispersion Parameter of Experiment 19 (CCl_4),
Period . 2
(--- Pasquill-Gifford)

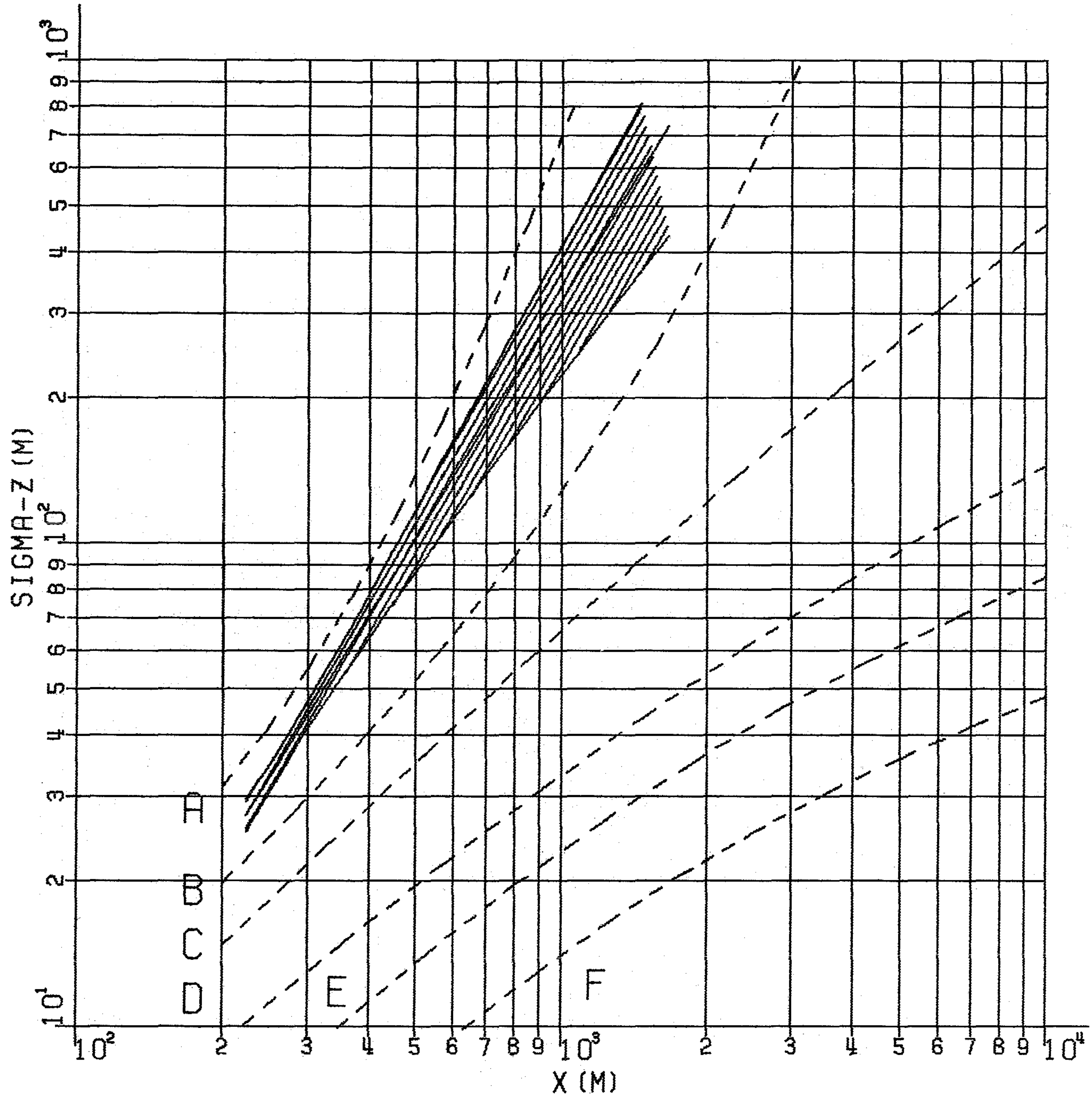

Fig. 19: Vertical Dispersion Parameter of Experiment 20 (CCl_4), Period 1
(--- Pasquill-Gifford)

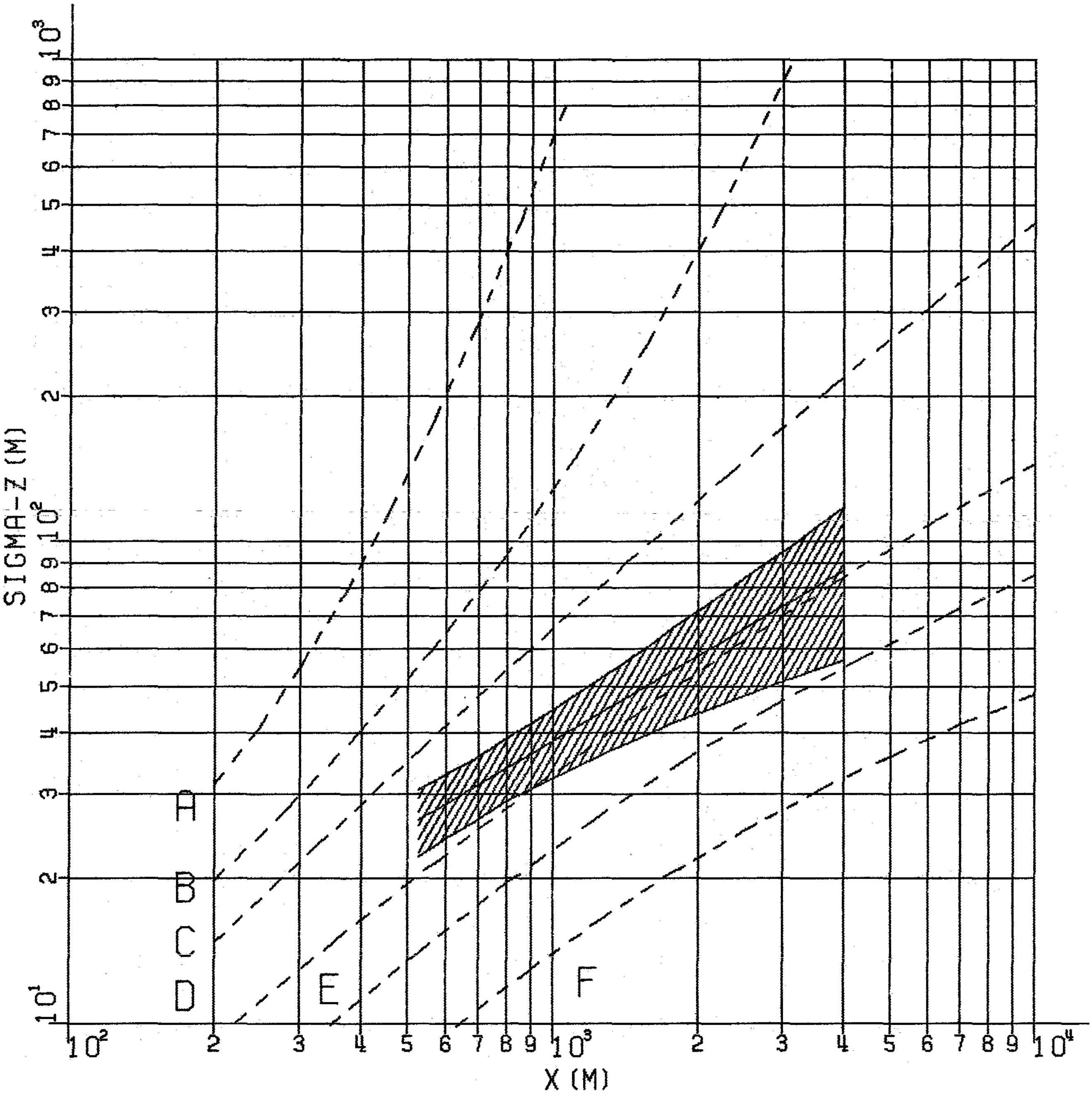

Fig. 20: Vertical Dispersion Parameter of Experiment 23 (HTO), Period 3
(--- Pasquill-Gifford)

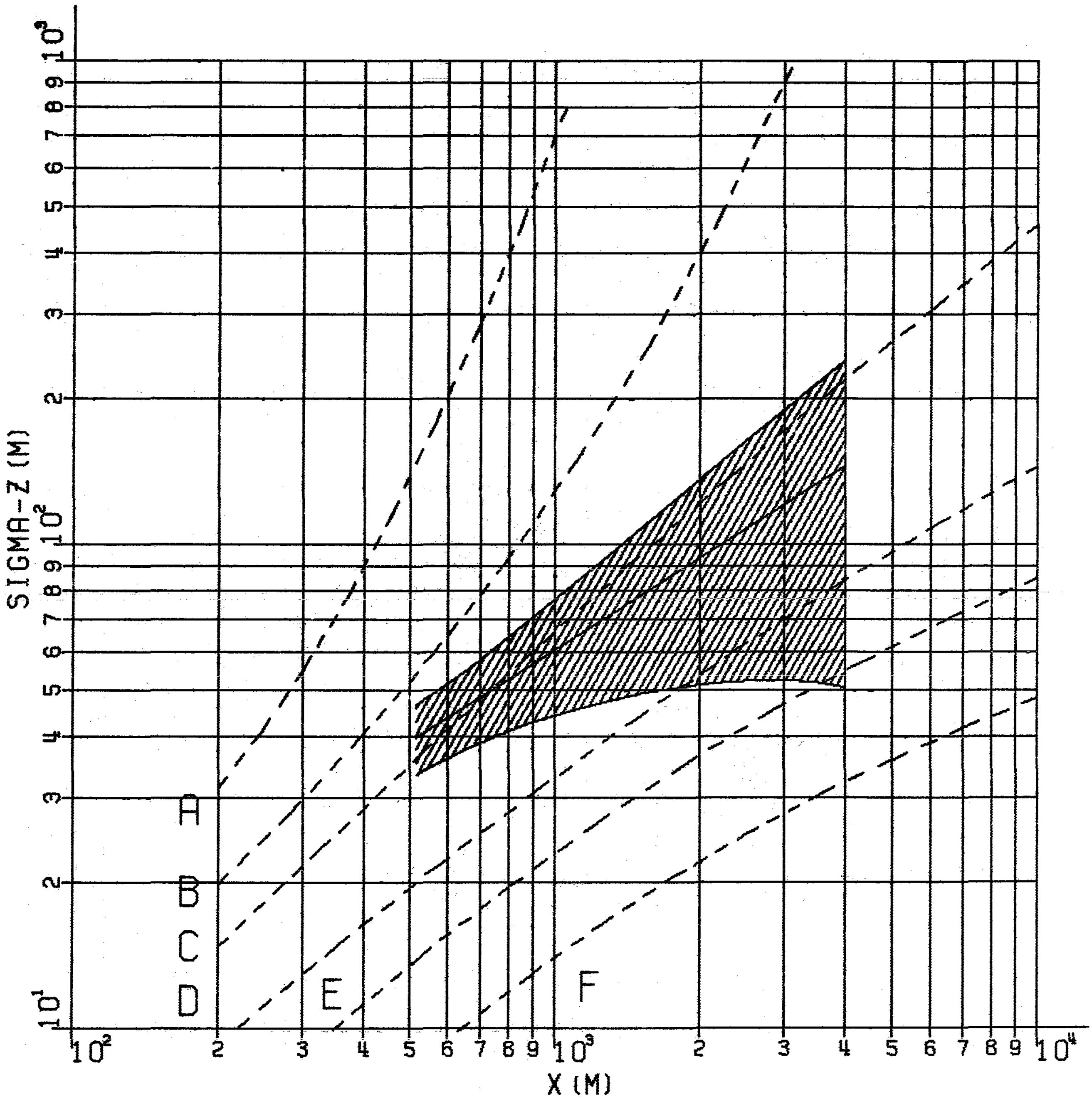

Fig. 21: Vertical Dispersion Parameter of Experiment 23 ($CFCl_3$), Period 3
(--- Pasquill-Gifford)

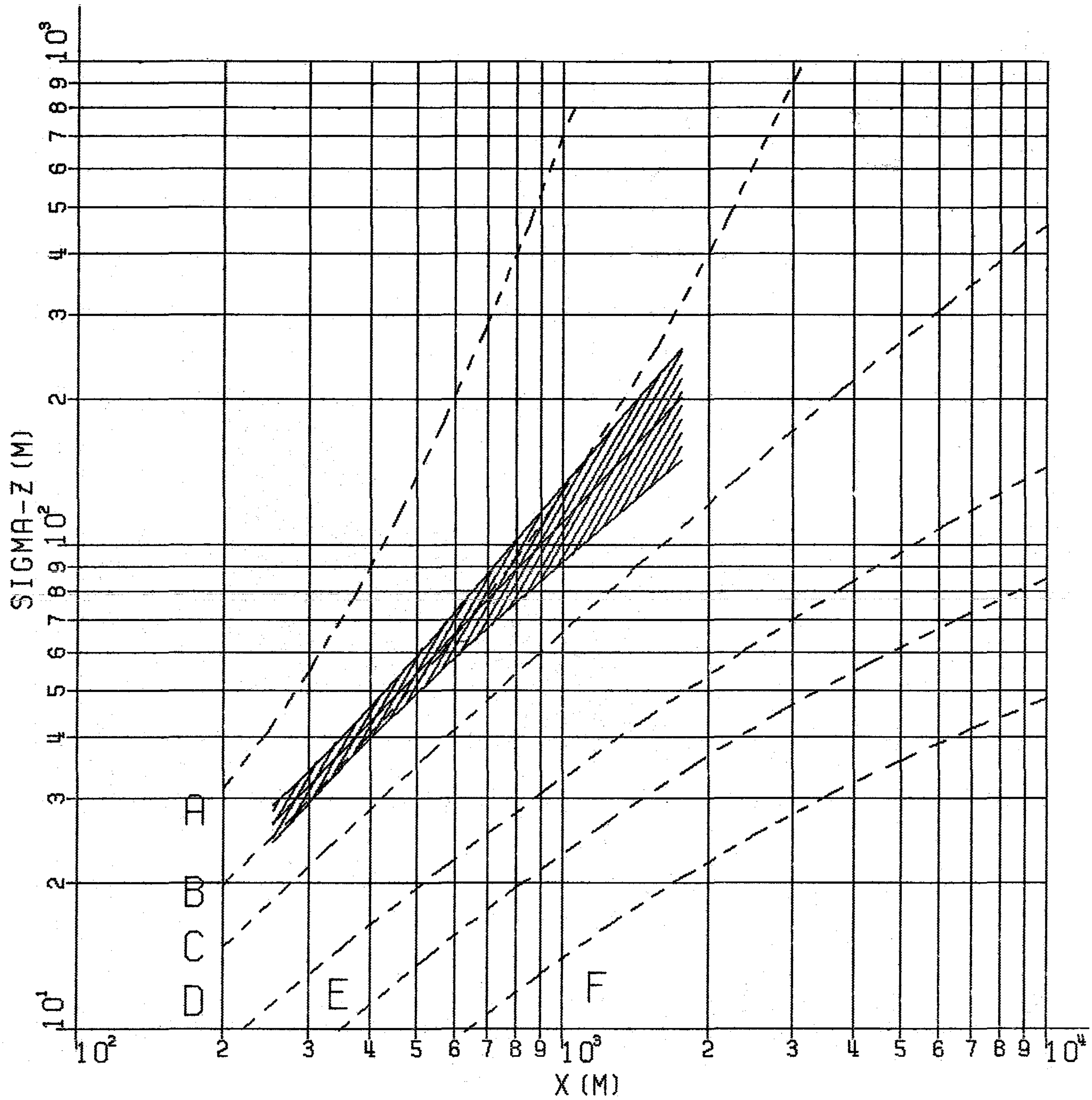

Fig. 22: Vertical Dispersion Parameter of Experiment 24 (HTO), Periods 1, 2
(--- Pasquill-Gifford)

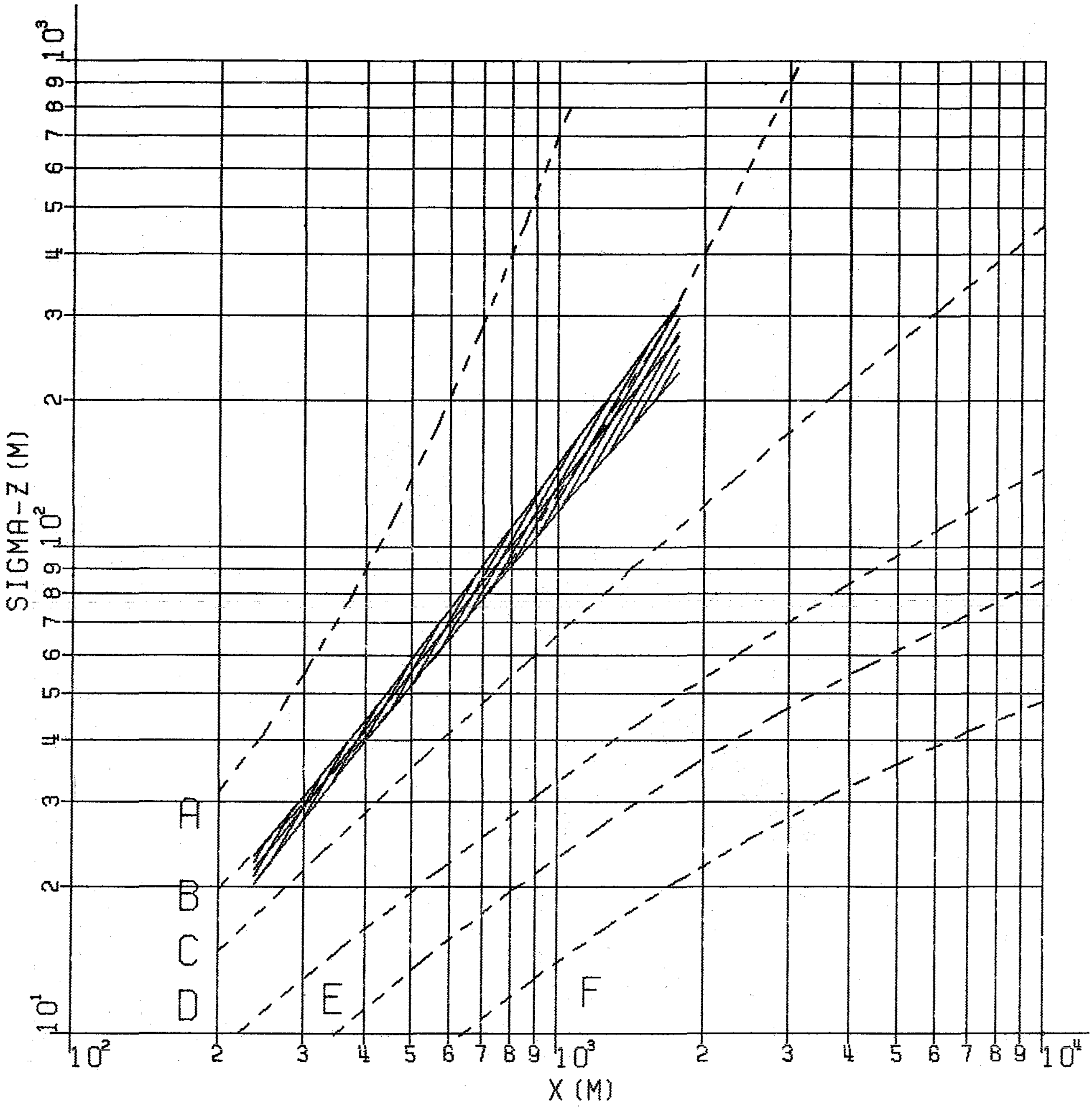

Fig. 23: Vertical Dispersion Parameter of Experiment 24 (CBr_2F_2), Periods 1, 2
(--- Pasquill-Gifford)

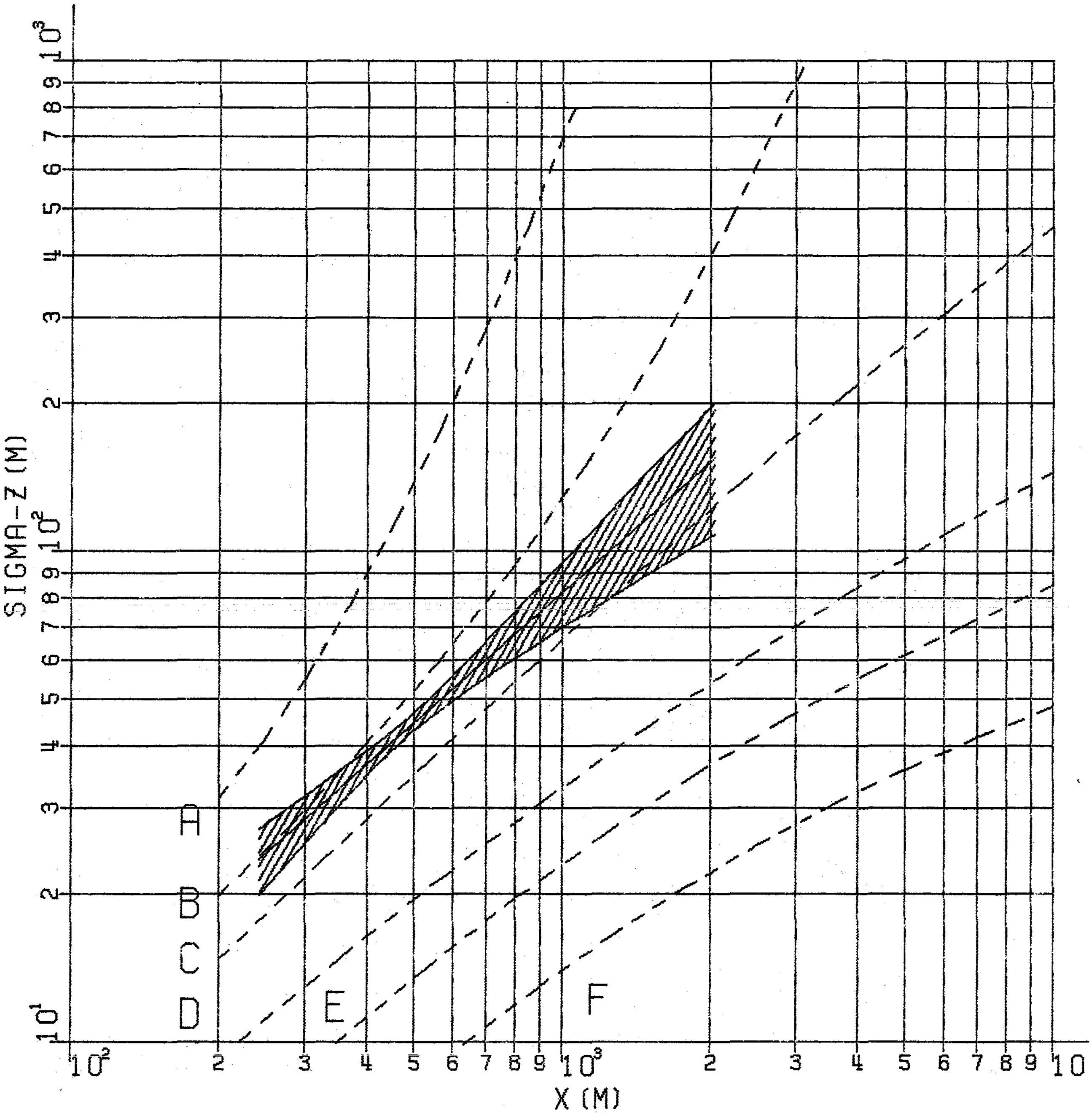

Fig. 24: Vertical Dispersion Parameter of Experiment 25 (HTO), Period 1
(--- Pasquill-Gifford)